REPUBLIC OF TURKEY

YILDIZ TECHNICAL UNIVERSITY

GRADUATE SCHOOL OF NATURAL AND APPLIED SCIENCES

EFFECT OF SALT BATHS CONTAMINATED WITH DIFFERENT CALCIUM COMPOUNDS ON CHEMICAL TEMPERING EFFICIENCY

Aslı ÇALI

MASTER OF SCIENCE THESIS

Department of Metallurgical and Materials Engineering

Program of Material

Advisor

Assoc. Prof. Dr. Ali Erçin ERSUNDU

February, 2021

REPUBLIC OF TURKEY

YILDIZ TECHNICAL UNIVERSITY

GRADUATE SCHOOL OF NATURAL AND APPLIED SCIENCES

EFFECT OF SALT BATHS CONTAMINATED WITH DIFFERENT CALCIUM COMPOUNDS ON CHEMICAL TEMPERING EFFICIENCY

A thesis submitted by Aslı ÇALI in partial fulfillment of the requirements for the degree of MASTER OF SCIENCE is approved by the committee on 26.02.2021 in Department of Metallurgical and Materials Engineering, Material Program.

Assoc. Prof. Dr. Ali Erçin ERSUNDU

Yıldız Technical University

Advisor

Approved by the Examining Committee

Assoc. Prof. Dr. Ali Erçin ERSUNDU, Advisor
Yıldız Technical University _____

Asst. Prof. Dr. Hakan YILMAZER, Member
Yıldız Technical University _____

Prof. Dr. Sevim İŞÇİ TURUTOĞLU, Member
İstanbul Technical University _____

I hereby declare that I have obtained the required legal permissions during data collection and exploitation procedures, that I have made the in-text citations and cited the references properly, that I haven't falsified and/or fabricated research data and results of the study and that I have abided by the principles of the scientific research and ethics during my Thesis Study under the title of Effect of Salt Baths Contaminated with Different Calcium Compounds on Chemical Tempering Efficiency supervised by my supervisor, Assoc. Prof. Dr. Ali Erçin ERSUNDU. In the case of a discovery of false statement, I am to acknowledge any legal consequence.

Aslı ÇALI

Signature

This study was supported by the Yıldız Technical University Scientific Research Fund under the project numbered FYL-2019-3683



To my family

and

all my friends.

ACKNOWLEDGEMENTS

Foremost, I would like to express my sincere gratitude to my advisor Assoc. Prof. Dr. Ali Erçin Ersundu for the continuous support of my MSc study and research, for his patience, motivation, discipline, and knowledge. His guidance helped me in all the time of research and writing of this thesis.

Secondly, I would like to thank Miray Çelikbilek Ersundu, who never refrained from her support during my MSc studies, helped me under all circumstances and made efforts to correct my deficiencies.

During my graduate education, I was one of the employees of Şişecam Science, Technology and Design Center, where I worked as an intern for a long time and where I conducted experimental studies of my thesis. I would like to express my sincere thanks to employees of the Surface Technologies Group, who contributed greatly to my experimental studies and interpretation of my experimental results, Dr. İlkay Sökmen, director of this group, Dr. Tuncay Turutoğlu, manager of this group, Dr. Burcu Öğüt, Ezgi Deniz Biçer, Beyza Yedikardeş and Emel Mercan, also Semin Atılgan, one of the researchers of the Analysis and Characterization Directorate and Yekta Ateş Gösterişlioğlu, one of the researches of the Melting Kinetics Directorate.

I would also like to thank Büşra Demir, Metallurgy and Materials Engineer, who was my biggest supporter in my experimental studies, with whom we did internship at Şişecam Science Technology and Design Center.

Finally, I would like to thank my beloved mother and father, Mualla Emir and Hayri Çalı, and my brother Özgür Çalı, who are always proud of me, who support me and increase my motivation even in times of difficulty.

Aslı ÇALI

TABLE OF CONTENTS

LIST OF SYMBOLS ..... **xi**

LIST OF ABBREVIATIONS ..... **xii**

LIST OF FIGURES ..... **xiii**

LIST OF TABLES ..... **xvi**

ABSTRACT ..... **xvii**

ÖZET ..... **xix**

1 Introduction **1**

1.1 Literature Review 1

1.2 Objective of Thesis 5

1.3 Original Contribution 5

2 Theoretical Information **7**

2.1 Structure of Glass 7

2.2 Mechanical Properties of Glass 12

2.2.1 Griffith's Theory 13

2.2.2 Theoretical Strength of Glass 14

2.2.3 Practical Strength of Glass 15

2.2.4 Flaw Sources and Their Removal 15

2.3 Glass Strengthening Methods 16

2.3.1 Removal of Surface Defects 16

2.3.2 Nullification of Surface Defects 17

2.4 Chemical Strengthening 20

2.4.1 Ion Exchange 22

2.4.2 Diffusion Mechanism 23

2.4.3 Stress Generation 26

2.4.4 Stress Relaxation 27

2.5 Corrosion of Glass 28
3 Experimental Studies 32
3.1 Sample Preparation 32
3.2 Chemical Tempering Process 33
3.3 Aging Process 35
3.4 Test and Characterization Studies 35
3.4.1 Surface Stress Characterization 35
3.4.2 Structural Analysis 35
3.4.3 Optical Analysis 36
3.4.4 Mechanical Analysis 36
3.4.5 Methylene Blue Test 38
3.4.6 pH Measurements 39
3.4.7 Alkalinity Tests 39
4 RESULTS AND DISCUSSION 41
4.1 Results for Pure KNO_3 Salt Bath 41
4.1.1 Compressive Stress and Depth of Layer Analysis Results 41
4.1.2 Vickers Hardness Test Results 41
4.1.3 Ring on Ring Test Results 41
4.1.4 Structural Analysis Results 42
4.1.5 Macro Examination Results 42
4.1.6 Optical Analysis Results 43
4.1.7 pH and Alkalinity Analysis Results 44
4.2 Results for $Ca(NO_3)_2$ Contaminated KNO_3 Salt Bath 44
4.2.1 Compressive Stress and Depth of Layer Analysis Results 44
4.2.2 Vickers Hardness Test Results 45
4.2.3 Ring-on-Ring Test Results 47
4.2.4 Structural Analysis Results 47
4.2.5 Macro Examination 48

4.2.6 Optical Analysis Results 49
4.2.7 pH and Alkalinity Analysis Results 50
4.3 Results of $CaCO_3$ Contaminated KNO_3 Salt Bath 51
4.3.1 Compressive Stress and Depth of Layer Analysis Results 51
4.3.2 Vickers Hardness Test Results 52
4.3.3 Ring-on-Ring Test Results 53
4.3.4 Structural Analysis Results 54
4.3.5 Macro Examination 55
4.3.6 Optical Analysis Results 56
4.3.7 pH and Alkalinity Analysis Results 56
4.4 Results of CaO Contaminated KNO_3 Salt Bath 57
4.4.1 Compressive Stress and Depth of Layer Analysis Results 57
4.4.2 Vickers Hardness Test Results 58
4.4.3 Ring-on-Ring Test Results 60
4.4.4 Structural Analysis Results 60
4.4.5 Macro Examination 61
4.4.6 Optical Analysis Results 62
4.4.7 pH and Alkalinity Analysis Results 63
4.5 Discussion 64
4.5.1 Evaluation of Compressive Stress and Depth of Layer Analysis Results 64
4.5.2 Evaluation of Vickers Indentation Test Results 67
4.5.3 Interpretation of Ring-on-Ring Test Results 69
4.5.4 Evaluation of Structural Analysis 71
4.5.5 Evaluation of Macro Examination Results 74
4.5.6 Evaluation of Optical Analysis Results 76
4.5.7 Interpretation of pH and Alkalinity Analysis 77

4.6 General Results and Future Outlook..... 79
REFERENCES..... 82
PUBLICATIONS FROM THE THESIS..... 87

LIST OF SYMBOLS

GPa	Gigapascal
MPa	Megapascal
σ	Strength
°C	Degree of Celsius
E	Young modulus
µm	Micrometer
Pa	Pascal
ɣ	Surface energy
J	Diffusion rate
D	Diffusion coefficient
v	Poisson's rate
cm	Centimeter
N	Newton
Pf(σ)	Failure probability
m	Weibull modulus
g	Gram
ml	Milliliter
mg	Milligram

LIST OF ABBREVIATIONS

NBO	Non-bridging oxygen
CS	Compressive stress
DOL	Depth of layer
PVB	Polyvinyl butyral
FTIR	Fourier transform infrared spectroscopy
HV	Vickers hardness
ppm	Parts per million
T_g	Glass transition temperature
XRF	X-ray fluorescence spectrometer
SLS	Soda-lime-silicate

LIST OF FIGURES

Figure 2.1 Schematic two-dimensional illustration of the atomic arrangement in a) Crystalline (long-range order) structure, b) Amorphous structure 8

Figure 2.2 Effect of temperature on the enthalpy of a glass-forming melt 8

Figure 2.3 Representative image of the SiO_4^{4-} tetrahedron 10

Figure 2.4 Network structure of a soda-lime silicate glass 12

Figure 2.5 A Schematic drawing of a Griffith's type flaw of length C and the effect which stress on bulk, σA, has on the stress at the crack, σc 13

Figure 2.6 Surface defect representation 14

Figure 2.7 Mechanism of chemical strengthening process 19

Figure 2.8 Comparison between the residual stress distributions in thermally and chemically strengthened glasses 20

Figure 2.9 Crack progression of un-strengthened and strengthened glass 21

Figure 2.10 General mechanism of residual surface compression increasing the fracture strength. 21

Figure 2.11 Glass corrosion mechanism a) (weathering) starts with a clean and uncorroded surface. (b) The formation of a water film occurs, due to the atmospheric conditions, allowing ionic exchange between the ions H^+ and H_3O^+ of water and the alkaline ions present in glass, which may be reinforced by the presence of acid gases. (c) This lixiviation reaction starts slowly but accelerates overtime; after the formation of a hydrated layer (light blue in the figure), rich in silica and alkaline oxides, (d) the glass surface becomes more resistant to the attack of water and the surface pH increases. The crystalline corrosion products (salts) stay in the glass surface after the water evaporates 30

Figure 2.12 The IR spectra of glass samples subjected to fastened corrosion test 31

Figure 3.1 Image of pre-cut samples ready for chemical tempering 33

Figure 3.2 Chemical tempering set-up (left: stainless steel basket containing glass samples, right: stainless steel box containing KNO_3 salt contaminated with different amounts of calcium compounds) 34

Figure 3.3 Schematic representation of the Vickers indentation technique 38

Figure 4.1 FTIR spectra of original glass and chemically tempered glass in pure KNO_3 salt bath before and after aging process 42

Figure 4.2 Macro photo of aged glass chemically tempered in pure KNO_3 salt bath 43

Figure 4.3 Macro photo of aged glass chemically tempered in pure KNO_3 salt bath after methylene blue test 43

Figure 4.4 Variation of CS and DOL values for glasses tempered in different amounts of $Ca(NO_3)_2$ contaminated KNO_3 salt bath 45

Figure 4.5 Vickers hardness test results of glass samples chemically tempered in different amounts of $Ca(NO_3)_2$ containing salts 46

Figure 4.6 FTIR spectra of original glass and glasses chemically tempered in pure (0 ppm) and $Ca(NO_3)_2$ contaminated (8 ppm) KNO_3 salt bath before and after aging process 48

Figure 4.7 Macro photos of aged glass samples chemically tempered in different amounts of $Ca(NO_3)_2$ containing salt baths 49

Figure 4.8 Macro photos of glass samples chemically tempered in different amounts of $Ca(NO_3)_2$ containing salt baths after methylene blue test 49

Figure 4.9 Transmittance and haze results of glasses chemically tempered in different amounts of $Ca(NO_3)_2$ contaminated salt baths 50

Figure 4.10 Variation of CS and DOL values for glasses tempered in different amounts of $CaCO_3$ contaminated KNO_3 salt bath 51

Figure 4.11 Vickers hardness test results of glass samples chemically tempered in different amounts of $CaCO_3$ containing salts 52

Figure 4.12 FTIR spectra of original glass and glasses chemically tempered in pure (0 ppm) and $CaCO_3$ contaminated (8 ppm) KNO_3 salt bath before and after aging process 55

Figure 4.13 Macro photos of aged glass samples chemically tempered in different amounts of $CaCO_3$ containing salt baths 55

Figure 4.14 Macro photos of glass samples chemically tempered in different amounts of $CaCO_3$ containing salt baths after methylene blue test 56

Figure 4.15 Transmittance and haze results of glasses chemically tempered in different amounts of $CaCO_3$ contaminated salt baths 56

Figure 4.16 Variation of CS and DOL values for glasses tempered in different amounts of CaO contaminated KNO_3 salt bath 58

Figure 4.17 Vickers hardness test results of glass samples chemically tempered in different amounts of CaO containing salts 59

Figure 4.18 FTIR spectra of original glass and glasses chemically tempered in pure (0 ppm) and CaO contaminated (8 ppm) KNO_3 salt bath before and after aging process 61

Figure 4.19 Macro photos of aged glass samples chemically tempered in different amounts of CaO containing salt baths 62

Figure 4.20 Macro photos of glass samples chemically tempered in different amounts of CaO containing salt baths after methylene blue test 62

Figure 4.21 Transmittance and haze results of glasses chemically tempered in different amounts of CaO contaminated salt baths 63

Figure 4.22 Breaking loads for glasses chemically tempered in pure KNO_3 and different calcium contaminated salts containing 8 ppm Ca^{2+} impurity ... 70

Figure 4.23 Weibull plot of glasses chemically tempered in pure KNO_3 and different calcium contaminated salts containing 8 ppm Ca^{2+} impurities 70

Figure 4.24 FTIR spectra of glasses chemically tempered in pure KNO_3 and different calcium contaminated salts containing 8 ppm Ca^{2+} impurity a) before and b) after aging process ... 73

Figure 4.25 Macro images of samples after aging process ... 74

Figure 4.26 Methylene blue test results of chemically tempered glass samples after aging process ... 75

LIST OF TABLES

Table 3.1 Chemical composition of glasses 32

Table 3.2 Amount of different Ca^{2+} containing compounds used in experimental studies 34

Table 4.1 Transmittance and haze test results of glass sample chemically tempered in pure KNO_3 salt bath 44

Table 4.2 pH and alkalinity results of pure KNO_3 salt bath 44

Table 4.3 Crack formation behavior of glass sample chemically tempered in 8 ppm $Ca(NO_3)_2$ contaminated salt bath 46

Table 4.4 pH and alkalinity test results for different amount of $Ca(NO_3)_2$ added salts 50

Table 4.5 Crack formation behaviors of glass sample chemically tempered in 8 ppm $CaCO_3$ contaminated salt bath 52

Table 4.6 pH and alkalinity test results for different amount of $CaCO_3$ added salts 57

Table 4.7 Crack formation behavior of glass sample chemically tempered in 8 ppm CaO contaminated salt bath 59

Table 4.8 pH and alkalinity test results for different amounts of CaO added salts 63

Table 4.9 CS and DOL results of glasses chemically tempered in different calcium contaminated salts 65

Table 4.10 Vickers indentation results of glasses chemically tempered in different calcium contaminated salts 67

Table 4.11 Crack formation behavior of glasses chemically tempered in 8 ppm Ca^{2+} containing salts 68

Table 4.12 Transmittance and haze results of chemically tempered glass samples in different calcium contaminated salts 76

Table 4.13 pH and alkalinity results of different salt baths 78

ABSTRACT

Effect of Salt Baths Contaminated with Different Calcium Compounds on Chemical Tempering Efficiency

Aslı ÇALI

Department of Metallurgical and Materials Engineering

Master of Science Thesis

Advisor: Assoc. Prof. Dr. Ali Erçin ERSUNDU

Glass is a material that is widely used in many industries thanks to its advantageous properties such as, transparency and high hardness, resistance to acidic and atmospheric factors and temperature changes. However, there are surface defects in glass resulting from its production method. These surface defects significantly reduce the strength of glass. Although there are different methods to increase the strength of glass the two mostly preferred methods in industry are thermal tempering and chemical tempering. Since thermal tempering cannot be applied to thin and complex shaped glasses, chemical tempering method is preferred in such glasses. In addition, thin, and durable glasses that provide higher strength to weight ratio as expected in the glass industry can be produced by chemical tempering method since the compression stress value obtained by this method is higher compared to thermally tempering method.

The parameters affecting the chemical tempering process should be taken into consideration in order to perform the chemical tempering process in a healthy way and to increase its efficiency. The main parameters are glass composition, process temperature, process time, salt bath composition, bath impurities and bath pH value. In this study, the effect of different calcium impurities i.e., $Ca(NO_3)_2$, $CaCO_3$,

and CaO – that can pass from glass composition to tempering salt during chemical tempering process – on chemical strengthening efficiency of commercial soda-lime silicate glasses was investigated in terms of mechanical, structural, and optical properties. In addition, corrosion behavior of glass samples was investigated by applying aging tests to the samples after chemical tempering process. Finally, the link between pH and salt contamination was investigated by analyzing the pH value of the chemical tempering bath.

As a result of the tests and characterization studies, it was observed that the calcium impurities in the chemical tempering salt caused a decrease in the compressive stress and depth of compressive stress layer of the glass samples, reduced the resistance to atmospheric corrosion by causing some change in the bond structures after the aging process and negatively affected the mechanical properties of the samples. In addition, it was concluded that calcium impurities in the salt bath did not affect the optical properties of the glass samples and did not significantly change the pH values of the salt bath. Based on these studies, it was concluded that the calcium impurities that may be present in the chemical tempering salt negatively affect the chemical tempering efficiency in terms of the structural and mechanical properties of glass samples.

Keywords: chemical tempering, salt bath contamination, salt bath composition, soda-lime silicate glass, thin glass, flat glass

ÖZET

Farklı Kalsiyum Bileşikleri ile Kirletilmiş Tuz Banyolarının Kimyasal Temperleme Verimliliğine Etkisi

Aslı ÇALI

Metalurji ve Malzeme Mühendisliği Anabilim Dalı

Yüksek Lisans Tezi

Danışman: Doç. Dr. Ali Erçin ERSUNDU

Cam, yüksek saydamlık başta olmak üzere, asidik ve atmosferik etkenlere ve sıcaklık değişikliklerine dayanıklı olması, yüksek sertliğe sahip olması gibi avantajlı özellikleri sayesinde pek çok sektörde yaygın olarak kullanılan bir malzemedir. Ancak, üretim yöntemi dolayısıyla camda yüzey hataları mevcuttur. Bu yüzey hataları, camın dayanımını ciddi oranda düşürmektedir. Camın dayanımını yükseltmeye yönelik pek çok farklı yöntem olmakla birlikte endüstriyel olarak en çok tercih edilen iki yöntem termal temperleme ve kimyasal temperleme yöntemleridir. Termal temperleme ince ve karmaşık şekilli camlara uygulanamadığından dolayı, bu gibi camların dayanımlarının arttırılması için kimyasal temperleme yöntemi tercih edilmektedir. Bunun yanı sıra, kimyasal temperleme yöntemiyle elde edilen basma gerilmesi değeri termal temperlemeye kıyasla daha yüksek olduğundan kimyasal temperlemeyle endüstride beklenen yüksek mukavemet/ağırlık oranını sağlayan ince ve dayanıklı camlar üretilebilmektedir.

Kimyasal temperlemenin sağlıklı bir şekilde yapılabilmesi ve veriminin arttırılabilmesi için kimyasal temperleme prosesini etkileyen parametreler göz

önünde bulundurulmalıdır. Bu parametrelerin başlıcaları, cam kompozisyonu, proses sıcaklığı, proses süresi, tuz banyosu kompozisyonu, banyo kirlilikleri ve banyo pH değeridir. Bu çalışmada, kimyasal temperleme işlemi boyunca camdan tuza geçebilecek $Ca(NO_3)_2$, $CaCO_3$, and CaO gibi farklı kalsiyum safsızlıklarının ticari soda-kireç silikat camların kimyasal temperleme verimine etkisi mekanik, yapısal ve optic özellikler açısından incelenmiştir. Bu kapsamda cam numuneler, kimyasal temperleme işleminden sonra mekanik, optik ve yapısal analizlere tabii tutulmuştur. Bunun yanı sıra, numuenelere yaşlandırma işlemleri uygulanarak kirliliklerin camların korozyon davranışına nasıl etki ettiği incelenmiştir. Son olarak, kimyasal temperleme banyosunun pH değeri analiz edilerek pH ve tuz kirliliği arasındaki bağlantı araştırılmıştır.

Yapılan test ve karakterizasyon çalışmaları neticesinde, kimyasal temperleme tuzunda bulunan kalsiyum kirliliklerinin, cam numunelerin basma gerilimi ve basma gerilim derinliği değerlerinde azalmaya sebep olduğu, yaşlandırma işlemi sonrası bağ yapılarında birtakım değişiklikler oluşturarak atmosferik korozyona karşı direncini düşürdüğü ve mekanik özelliklerini olumsuz yönde etkilediği gözlemlenmiştir. Bu çalışmalara dayanarak, kimyasal temperleme tuzunda bulunabilecek kalsiyum kirliliklerinin, kimyasal temperleme verimini, cam numunelerin yapısal ve mekanik özellikleri yönünden olumsuz etkilediği sonuçlarına varılmıştır.

Anahtar Kelimeler: kimyasal temperleme, banyo kirliliği, tuz kompozisyonu, soda kireç silikat camı, ince cam, düz cam

1
Introduction

1.1 Literature Review

Glass is one of the strongest human-made material, but surface defects that occur during the manufacturing process lowers its strength [1],[2]. Therefore, the strength of glass in practice is much lower than its theoretical value. These surface defects act as stress concentrators by raising local stresses to levels that exceed theoretical strength and cause glass breakage [3]. Several different phenomena have been proposed regarding how surface microcracks occur in glasses. These can be listed as cooling stresses, spontaneous crack formation, chemical effects and many other factors. However, it is well known that the majority of surface defects that lower the strength are micro-cracks caused by mechanical damage during manufacture, processing and use of glass [4]. Griffith is the first to suggest that the low strength of glass may be predominantly related to the surface. According to Griffith's theory on brittle materials such as glass and ceramics, mechanical strength depends on the shape and size of the surface defects. Defects significantly reduce the theoretical strength of the glass. In other words, imperfections on the glass surface are much more important than mass. This indicates that any intervention must begin on the glass surface for a decisive improvement in the strength of the glass. Therefore, glass strengthening studies are mainly aimed at removing the effects of microscopic surface defects [5].

Technologically successful glass strengthening techniques are methods that inevitably accept the presence of surface damage but eliminate its negative effect. These methods are coating, lamination, thermal tempering, and chemical tempering. Among these methods, commercially most preferred ones are thermal and chemical tempering. In thermal tempering, the glass material is rapidly cooled from a temperature above the glass transition temperature. Due to the rapid cooling, a temperature difference occurs between the inner parts and the surface of the glass.

In this way, while a tensile stress occurs in the inner parts, a compression stress occurs on the surface. On the other hand, chemical tempering is based on immersion of glass containing smaller alkali ions into a molten salt containing larger alkali ions and alkali ion exchange by mutual diffusion mechanism. At a temperature below the glass transition temperature, the small alkali ions in the glass immersed in the molten salt bath are replaced by large alkali ions in the salt, and thus a compressive stress layer is formed on the surface. Therefore, the compression stress directly depends on the number of ions exchanged. The depth of the modified layer depends on the processing time and temperature, as a determining parameter for strengthening. Both methods are based in principle on producing a compressive stress that prevents the formation and propagation of defects and cracks on the glass surface. Thermal tempering is based on the cooling rate gradient across the glass thickness and glass production at different temperatures. This technique is accomplished by rapid cooling from a temperature above the glass transition temperature. Therefore, this processing procedure cannot be applied to glass with low thermal expansion, hollow shape, complex shape or thinner than 2 mm [6]. In addition, chemical tempering method has advantages such as creating a relatively higher compressive stress and no measurable optical distortion on the surface. With the chemical tempering method, it is possible to produce thin and light glasses with high strength/weight ratio that is accepted as an important parameter in the industry.

Ion exchange has been used to change the color of glass for hundreds of years [7],[8]. The ion exchange process to strengthen the glass was first suggested by Kistler [9] and Acloque and Tochon [10] in 1962. However, first chemical tempering was carried out in the 1970s to improve the mechanical properties of glasses containing alkali ions [11]. Since then, the chemical tempering method has been widely used because it provides higher compressive stress compared to other strengthening methods such as thermal tempering. Today, this method has been developed and used in many industries such as for aircraft cockpit windshields, transparent armors, solar panels, exterior glasses, glass containers, automatic injector cartridges, photocopy glasses, and thin screens (monitors, mobile phones, and tablets) [12].

In order for chemical tempering to be performed efficiently, it is necessary to know the parameters that this method is affected by. The main factors affecting chemical tempering can be explained as follows.

1. Glass Composition: Chemical tempering is applied only to glasses containing sufficient alkali ions. There are studies in the literature regarding the effect of glass composition on chemical tempering efficiency. For example, Fu and Mauro [11] found that ion-exchanged aluminosilicate glasses undergo more network expansion than soda lime glasses, so aluminosilicate glasses provide a much better environment for chemical strengthening through ion exchange. While aluminosilicate glasses used in their study can reach compression stress values higher than 1 GPa, soda lime glasses have reached a maximum compression stress value of 500 MPa. In addition, they found that in aluminosilicate glasses, the mutual diffusion coefficient is higher and thus the efficiency of the chemical tempering process is higher. In addition, there are other studies showing that borosilicate glasses with low thermal expansion coefficient and glasses containing PbO have low chemical tempering efficiency.

2. Process Temperature: Chemical tempering process takes place by diffusion mechanism. Since temperature is an important parameter that affects diffusion, it also affects the efficiency of the chemical tempering process. As the temperature increases, the diffusion rate and chemical tempering efficiency increase. However, temperature can also cause stress relaxation in glasses. To avoid this effect, the temperature should not be too high. If the temperature reaches the glass transition temperature range, the network structure of the glass is distorted, and the bond forces are loosened [13]. Therefore, the temperature should be chosen high enough to allow the mutual diffusion of ions in the glass and the ions in the salt, but low enough not to cause stress relaxation.

3. Process Time: Since chemical tempering process is carried out by diffusion mechanism, time also has an effect on efficiency. When the time is too much like temperature, it can cause stress relaxation, so it must be kept at an optimum level.

4. Salt Bath Composition: Salt bath composition also has important effects on chemical tempering. For example, Sglavo et al. [12] found that small differences in

potassium nitrate salt bath composition play an important role in the strengthening process of soda-lime silicate glass by ion exchange. They used three different KNO_3 salts commercially available for industrial use and a salt from an unknown source that had previously been used for at least 1000 hours in different Na^+-K^+ ion exchange processes and observed that the chemical tempering efficiency changed. However, it is difficult to make a clear judgment here, as other impurities in salt must be examined one by one. In addition, Varshneya and Spinelli [14] carried out chemical strengthening processes in salt baths with $NaNO_3$:KNO_3 composition using salt compositions in molar ratios ranging from 5:95 to 50:50 on lithium aluminosilicate glass. They showed that the highest strength was obtained in the salt mixture using 20 mol% $NaNO_3$.

5. Salt Bath Contamination: The literature studies conducted so far show that the contamination of the salt bath by the ions passing through the glass over time affects the chemical tempering efficiency. When these impurities accumulated in salt are above a certain amount, they pass from the salt bath to the glass and prevent ion displacement. This effect is called the blocking effect. On the other hand, in other studies in the literature, it has been shown that the presence of alkali or alkaline earth impurities is responsible for "poisoning" the melt salt or "blocking" the ion exchange. Frischat [15] summarized several experimental findings showing that the balance between salt bath and glass can be significantly affected by small amounts of alkali ions in the bath. Kolitsch et al. [16] analyzed the ion exchange process of Na_2O-$0.35Al_2O_3$-$2SiO_2$ glass containing a small amount of alkaline earth ions and observed that Ba, Sr and Ca block Na^+-K^+ exchange. In particular, Ca, although it was present in the solution in concentrations as low as 0.05 mol%, significantly prevented the ion exchange. It has been determined that ion exchange stops effectively for Ca concentrations exceeding 5 mol%. Zhang et al. [17] showed that Na^+-K^+ ion exchange in a soda-lime-silicate glass immersed in KNO_3 can be blocked by Ca, Sr, Ba, and Na ions in the molten salt bath. In their study, it was observed that even low Ca concentrations of 0.01 mol% are sufficient to limit the change. Sglavo [18] reported that the presence of Na impurity in salt does not appear to be a critical problem, at least up to a concentration of about 0.5% by weight. In contrast, the presence of very small amounts (even below 100 ppm) of alkaline earth ions such

as Ca, Mg was found responsible for limiting the ion exchange process, by activating a kind of blocking effect on the surface for Na^+-K^+ exchange. Therefore, the composition of the salt needs to be controlled very carefully. Demir [19] reported that Na_2O, $NaNO_3$, Na_2CO_3 and $NaHCO_3$ impurities, which are likely to be present in the chemical tempering salt, should be below 500 ppm in order not to affect the chemical tempering efficiency.

6. pH of the Salt Bath: Although there are references to the pH effect in the literature, no detailed investigation has been made in this context.

Taking all these effects into consideration, in this study, research has been carried out on the effect of salt bath contamination, which is one of the crucial parameters that affect the efficiency of chemical tempering process.

1.2 Objective of Thesis

The objective of this thesis is to examine the effect of bath contamination through different forms of calcium impurities, i.e. $Ca(NO_3)_2$, $CaCO_3$, and CaO, on chemical tempering efficiency of commercial soda-lime silicate glasses in terms of mechanical, structural, and optical properties. In addition, it is aimed to observe the corrosion behavior of glass samples after chemical tempering process and understand the relationship between pH value and bath contamination.

1.3 Original Contribution

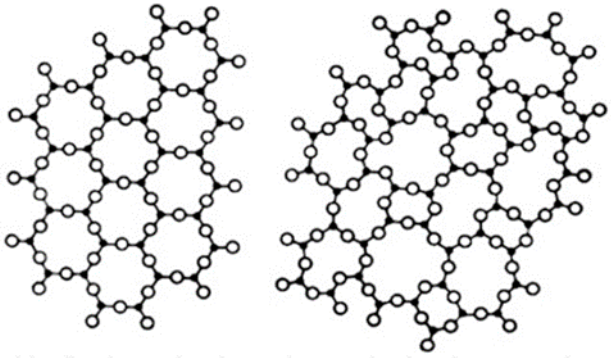
There exist several studies in the literature searching the effect of salt contamination on chemical tempering. However, these studies are limited to the investigation of blocking effect and are not comprehensive and systematic. The forms in which these impurities pass into salt are also important and should be considered. The contamination forms that have been investigated so far are usually the nitrate forms of the elements. In this study, different from the current literature, in addition to nitrate forms, oxide and carbonate forms of calcium impurities were studied. It is also thought that bath contamination has a proportional relationship with bath pH. However, there is no study revealing the link between pH and bath contamination in the literature. Therefore, in this study, the connection of the change in the pH of the salt bath with the contamination was also investigated. Considering all these

aspects, this study aims to improve existing bath contamination studies and to propose measures to eliminate the negative effects of contamination on chemical tempering process. All these working steps listed are unique in themselves.

2
Theoretical Information

2.1 Structure of Glass

Glass is a high-viscosity, brittle solid produced by cooling the molten material so that the internal arrangement of atoms or molecules remains in a random or irregular state similar to the arrangement in a liquid. The brittle properties of glass can be explained by the fact that the bonds between the atoms that form the network structure have strong elastic properties and allow very low amounts of plastic deformation, and thus, cracks occur when the directional covalent bonds between the atoms are broken without being able to change their angles. Glass does not crystallize while cooling from the melt to the solid state. For this reason, glass is an amorphous material. Amorphous materials, unlike those with crystalline structure, do not have an ordered structure that repeats continuously and has a short distance structure. This means glasses are materials that only show a regular structure in terms of nearby particles but lack the long-range order of crystals. [20]-[22]. The representative image of the network structure of crystal and amorphous materials is given in Figure 2.1.



a) b)

Figure 2.1 Schematic two-dimensional illustration of the atomic arrangement in a) Crystalline (long-range order) structure, b) Amorphous structure [23]

The characteristic property of the glasses is that they show glass transition, which is a reversible transition from a solid, hard state to a melted or rubber-like state. This happens at a temperature range, not a constant temperature. The glass transformation behavior is defined on the basis of enthalpy versus temperature diagrams as shown in Figure 2.2. [21].

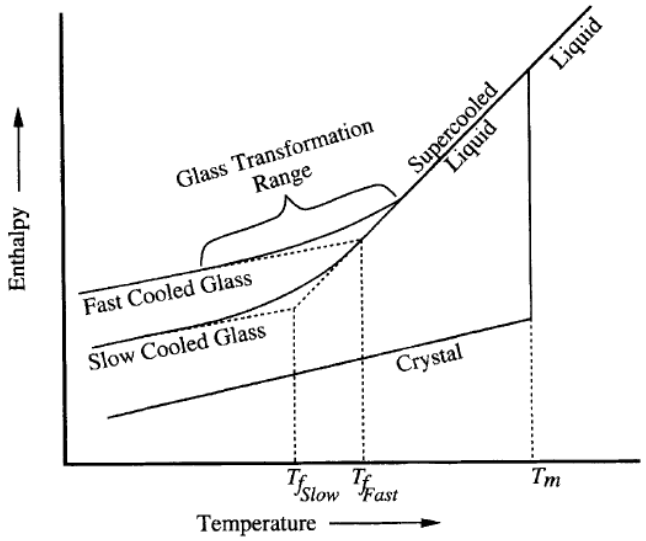


Figure 2.2 Effect of temperature on the enthalpy of a glass-forming melt [3]

Cooling to any temperature below its melting temperature normally causes the material to crystallize and a long-range, periodic atomic arrangement to form. When

this occurs, the enthalpy suddenly drops to the appropriate value for the crystal. Continuing to cool the crystal causes further decrease in enthalpy due to the crystal's heat capacity. If the material can be cooled quickly enough, the atoms cannot form a regular structure in the liquid phase and freeze in their position. The enthalpy begins to deviate from the equilibrium line following a gradually decreasing slope curve until it is eventually determined by the heat capacity of the frozen liquid. In this case, amorphous glass with a short distance arrangement is formed. The temperature zone corresponding to the enthalpy where the liquid and frozen solid are in equilibrium is known as glass transformation region. [3]

Glass structure generally consists of oxides with various functions. Various models have been proposed to define the glass structure [24]. The most commonly used models for glass structures today are based on the original ideas of Zachariasen [25], who classifies the oxides in three categories: glass formers, modifiers, and intermediates according to their function in the formation of glass.

The basic building blocks of oxide glasses are SiO_2, B_2O_3, GeO_2, P_2O_5 and As_2O_3 tetrahedral. They have strong bonds and form the network structure of the glass and are called network formers. The network formers, for example SiO_2, can form glasses themselves without adding another oxide and they are main components in the structure of glassy material. Silicon oxide is called the network former because it forms the structure of the glass called the glass matrix. Other oxides that are included in the composition of the glass are classified according to their effects on the formation of the glassy structure. These are; ''network modifiers'' and ''intermediates''. Different types of alkali metals and alkaline earth metals such as Na_2O, Li_2O, K_2O, CaO, MgO, SrO and BaO, commonly referred to as network modifiers. They are added to change the physicochemical properties of the glass, most importantly, reducing the softening point to simplify production. These are found in the form of loosely bound monovalent and bivalent ions in glass. Network modifiers disrupt network structure. Glass strength can be increased by inserting products called network intermediates such as ZnO, Al_2O_3, CdO, TiO_2 and PbO into the glass matrix. Although network intermediates cannot form the glass matrix on their own, they contribute to glass strength. Intermediates may have a disruptive

effect on the network structure, or they can also be included in the network structure depending on the composition of the glass. For example, aluminum is trivalent and replaces the 4^- valence silicon atoms. This disrupts the formation of a regular silicon oxide crystal, causing an amorphous network [21],[26],[27],[28].

Glasses that use SiO_2 as glass former in the production of glass are called silica-based or silicate glasses. Silicate glasses consist of a topologically irregular network of silicon and oxygen atoms. SiO_2 is the most commonly used oxide in glass production because it is easy to find among glass-making oxides and is a good glass former. SiO_2 has a tetrahedral structure consisting of silicon and oxygen atoms. SiO_4^{4-} tetrahedron is formed by surrounding Si^{4+} in the center of the structure with O^{2-} ions, and SiO_4^{4-} tetrahedron is the basic building unit of silica-based glass material. The representative image of the SiO_4^{4-} tetrahedron is given in Figure 2.3. Two Si^{4+} ions share an O^{2-} ion and form a three-dimensional network structure connected at the corners. This oxygen, which connects tetrahedrons, is called bridging oxygen.

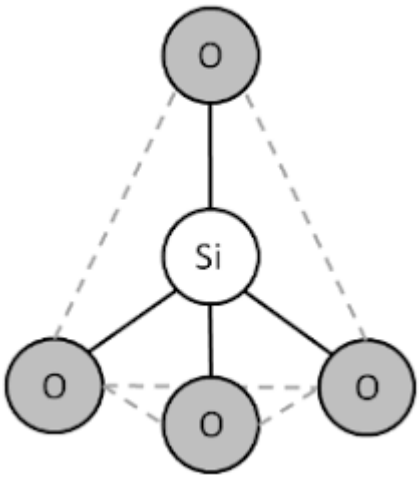


Figure 2.3 Representative image of the SiO_4^{4-} tetrahedron [29]

Due to the strong bond between Si^{4+} and O^{2-} ions, the movement capabilities of ions are very limited. As a result of rapid cooling of the SiO_2, which has a very high viscosity in the molten state, below the melting temperature, the ions cannot find enough time to regulate and a glassy structure occurs as a result of the random dispersion of tetrahedra within the structure. The fact that the bond angles of the tetrahedra in the glass structure are not constant causes irregular and different size

interstitial spaces in the structure. Other ions that participate in the SiO_2 structure are usually freely located in these spaces.

SiO_2, which is a good glass maker, increases the viscosity and melting temperature of glass, as well as its chemical resistance and thermal shock resistance. Network structure-modifying oxides such as Na_2O, K_2O, CaO are added to the composition in certain proportions depending on the physical and chemical properties required in the glasses or some factors required by the production conditions of the glass. Numerous modifying oxide ions incorporated in the structure are generally located in the gaps in the network structure, which causes the electric charge to be balanced by causing the Si–O bonds to break and oxygen ions that do not bridge the structure to form [27],[30].

The effects of the components on the glass properties in soda-lime-silicate glasses are given below:

With the increase in the amount of SiO_2 (silica), the melting temperature of the glass increases, its strength increases and its expansion decreases. By increasing the amount of soda (sodium oxide - Na_2O), the melting temperature of the glass decreases, its strength decreases, and the thermal expansion of the glass increases. If the amount of CaO is increased, glass with higher chemical resistance is obtained, leading to high levels of calcium oxide devitrification problem. Therefore, very care must be taken in following the compositions in which the CaO level is raised. [27],[30],[31].

The network structure formed by adding Na_2O and CaO to silica-based glasses is as shown in Figure 2.4. There is a network of silicon dioxide molecules in the core of a soda-lime glass. Among them, calcium and sodium ions are embedded. When sodium oxide (Na_2O) is introduced into the structure of the glass in the melting process, the resulting network connections are reduced due to excess oxygen. Thus, non-bridging oxygen (NBO) occurs [32].

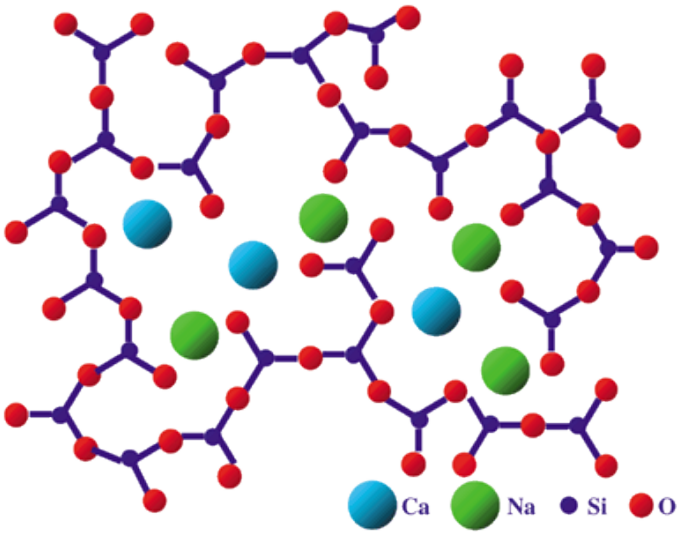


Figure 2.4 Network structure of a soda-lime silicate glass [33]

Glass is an important material which is used in many industries due to its advantageous properties such as transparency, high hardness, high chemical stability, form stability, formability, relatively low price and recyclability. The mechanical strength of glass mainly depends on the distribution of defects in the glass surface and surrounding environmental factors causing surface defects. The use of glass is limited by its unreliable mechanical properties and brittle nature [22]. For these reasons, the strength of the glass should be increased. In order to carry out studies to increase the strength of glass, firstly, the mechanical properties of the glass must be known.

2.2 Mechanical Properties of Glass

Glass is a brittle material, and its mechanical toughness is low. The usage areas of glass are limited due to being mechanically brittle. Based on the bonding energies of network formers, for example SiO_2, pristine glass should have a much higher strength than observed. The theoretical mechanical strength of a soda-lime silicate glass (the stress that the glass is exposed at the moment of breaking) is around 7000 MPa due to the very strong chemical bonds between silicon and oxygen that make up the network. Theoretical strength is the strength of the glass, which is perfectly homogeneous and does not contain defects on its surface. However, inherent defects on the glass surface (sub-micron and micro-cracks) or defects on the surface with external factors reduce the mechanical strength of the glass up to about 1% of the

theoretical strength [34]. Especially pristine glass is reported to be strong, but due to defects during production, this strength decreases to approximately 35-70 MPa [1].

Based on the work of Inglis and Griffith, it is now well established that sharp tipped flaws (generally referred to as ''Griffith Flaws'') are present on the surface of the entire glass (due to manufacturing and handling), and these flaws act as stress raisers when loads are applied (see Figure 2.5) [35].

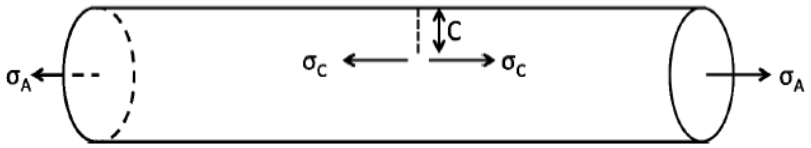


Figure 2.5 A Schematic drawing of a Griffith's type flaw of length C and the effect which stress on bulk, σA, has on the stress at the crack, σc [36]

2.2.1 Griffith's Theory

Many years ago, Griffith (1921) introduced a fundamental theory that explained the fragility of glass. He presumed the presence of small, crack-like flaws in all materials. The stress-concentrating effect of these flaws is insignificant in ductile materials because a small amount of flow in the region of the crack tip relieves the local over-stressed condition. However, brittle materials do not have this option and crack propagation occurs even when a small amount of load is applied, resulting in fracture and failure. Many suggestions have been made about the way surface microcracks appear. Spontaneous crack formation due to cooling stresses, chemical effects and many other effects is indicated. However, there is convincing evidence that most surface structures that decrease strength are microcracks caused by accidental mechanical damage during manufacture, processing and use [37].

The calculation of theoretical strength of glass by Inglis [38] agrees with the assumption by Griffith [39],[40]. In other words, calculation was made by assuming that there are microscopically small surface flaws in the glass. These surface flaws act as stress concentration centers when any tension is applied to the glass.

Consequently, in practice, surface flaws have a dominant influence on effective strength of glass [5].

Other mechanical properties of glasses are due to the nature of the material. The elastic modulus, E, is determined by the bonds in the network structure of the glass. The hardness of glasses is a function of the strength of individual bonds and the density of packing of the atoms in the structure. However, the fracture behavior of glasses is generally determined by the environmental factors, not by the natural strength of the bonds that make up the glass structure [3].

Typical surface flaws on the glass surface (see Figure 2.6) are usually between 1 and 10 μm. These flaws significantly reduce the mechanical strength of the glass. The following theory derived from Griffith provided the basis for understanding the mechanical strength of brittle materials such as glass. It is based on energy and explains how flaws affect mechanical strength.

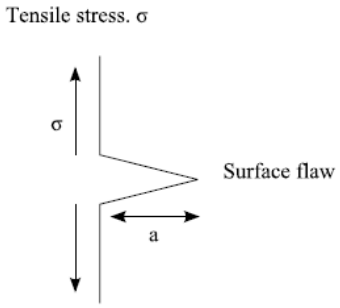


Figure 2.6 Surface defect representation [20]

$$\sigma_c = \sqrt{\frac{2E\gamma_s}{\pi a}} \tag{2.1}$$

where σ_c is the stress required for crack propogation (Pa), E is the Young's Modulus (Pa), γ_s is the specific fracture surface energy (J/m^2) and a is the depth of surface defect (m) [34].

2.2.2 Theoretical Strength of Glass

Orowan suggested that the stress needed to break a bond is determined by the energy required to create two new surfaces due to fracture. The Orowan stress, σ_m, is given by the expression:

$$\sigma_m = \sqrt{\frac{E\gamma}{r_o}} \tag{2.2}$$

where ɣ is the fracture surface energy having a value in the range of 2 to 4 J m^{-2}. E is the elastic modulus, and r_o is the atomic separation distance at equilibrium spacing of the atoms. Since the terms in this expression are all relatively independent of the glass composition, we estimate that glasses, regardless of their composition, should have strengths in the range of 1 to 100 GPa. The strength value calculated with this equation is called theoretical strength.

2.2.3 Practical Strength of Glass

The strength value calculated from the above equation is much higher than the strength value obtained in practical applications of bulk glasses. This reduction in strength is based on the presence of flaws on the surface of the glass. These surface flaws act as stress concentrators, raise local stresses to levels that exceed theoretical strength and cause glass fracture. Griffith studied this problem in detail and derived the following equation.

$$\sigma_f = \sqrt{\frac{2E\gamma}{\pi c^*}} \tag{2.3}$$

where σ_f is the failure stress and c* is the critical crack length for crack growth.

Surface flaws caused by external factors are not material specific defects. For this reason, the inherent strength of a glass is usually of little importance in determining practical strength.

2.2.4 Flaw Sources and Their Removal

Surface defects may occur on the glass for various reasons. For example, contact of glass with any harder material may cause a defect. When the glass comes into contact with a hard material, abrasion may occur on the surface, which reduces the strength of the glass. In fact, contact with another piece of the same glass or metal objects used to process the glass is sufficient to create a defect. Chemical attack can also generate defects. Touching a glass with your fingertip causes defects through attack on the surface due to NaCl passing through the skin. Thermal stresses that

occur during the rapid cooling of a glass can result in defects caused by thermal shock. The strength of glasses that are heated for a long time also decreases by forming a small number of surface crystals or adhering dust particles to the glass surface [5].

Consequently, Griffith explained the reason for the low strength of the glass with the presence of a large number of small, semi-elliptical surface flaws, now called Griffith flaws. When the glass is loaded, it starts to break from these surface flaws before the part that does not contain the defects. As a result, deficiencies on the glass surface are much more important than deficiencies on the inside of the glass. Therefore, any attempt to increase the strength of the glass should start from the surface. There are many studies in this context [3].

Flaws can be removed by removing the outer surface of the material by chemical etching or mechanical polishing. Etching blunts the flaw tip and reduces the flaw length, while polishing simply reduces the length of the flaw to below the Griffith criterion. Flame polishing removes flaws through viscous flow in the near surface region. Also, flaws can be nullificated via coating, lamination, thermal tempering or chemical tempering [5].

2.3 Glass Strengthening Methods

As can be seen, since the most important reason for the low mechanical strength of the glass is surface defects, the processes for increasing the strength of the glass should start from the glass surface. In this context, the methods used to eliminate the negative effects of surface defects can be grouped under two main headings. These are removal of surface defects and nullification of surface defects.

2.3.1 Removal of Surface Defects

One of the procedures that can be done to eliminate the negative effects of surface defects is to remove it. The methods applied under this heading fall into two different categories.

1. Mechanical Polishing

In the mechanical polishing process, the surface is abraded into small particles using a grinding matter. Mechanical polishing substrates always get rough, but this degree of roughness can be controlled to some extent. Polishing simply reduces the length of the flaw to below the Griffith criterion [41].

2. Etching with HF and Other Agents

In this method, the outer surfaces of the glass, including microcracks, are removed using hydrofluoric acid or other chemical agents. Etching blunts the flaw tip and reduces the flaw length. The strength of the glass increases quickly at first and then more slowly [37].

Removal of defects is effective only for short periods, since new defects are easily formed. For this reason, nullification methods, which are more effective than these methods, are applied.

2.3.2 Nullification of Surface Defects

Nullification methods focus on preventing the formation of new cracks and preventing the growth of existing cracks.

1. Coating

During the shaping and annealing of glass sheets, intensive studies are carried out to prevent surface defects with special, permanent or temporary protective coatings. These coatings must be abrasion resistant and protect the glass surface from ambient environment and mechanical contacts. Although the strength of glass can be increased up to 300-500 MPa with coating methods, the strength decreases if the coating is worn or rubbed off due to storage conditions or other atmospheric reasons [42]. Coating methods can be applied to prevent the formation of cracks, but they also have limited effect.

2. Lamination

Laminated glass is made by gluing the PVB (polyvinyl butyral) resin glue film between two or more glass sheets, then by heating, pressing and bonding them to form a flat or curved glass product compound.

If we accept the fact that defects will present, we must focus on preventing crack growth. Since crack growth requires the presence of a tensile stress at the end of the defect, the creation of the compression zone near the surface prevents crack growth. Growth does not occur until the applied stress is large enough to overcome residual compressive stress and produce a tensile stress at the crack tip [3]. There are two methods used to produce compression stress on the surface. These; thermal tempering and chemical strengthening

3. Thermal Tempering

Thermal tempering is based on the formation of compressive stress on the surface due to the fact that the inside and the surface of the glass have different cooling rate during the rapid cooling of the glass from a temperature above the glass transition temperature. During this process, the glass surface will solidify very quickly, and the interior of the glass will continue to shrink. In this way, while compressive stress occurs on the surface of the glass, tensile stress occurs in the interior parts to compensate for this compression [5]. The stress value (compressive stress, CS) and thickness (depth of layer, DOL) of the compression layer that will be formed on the glass surface by the thermal tempering method are affected by the cooling rate, thickness and thermal expansion coefficient of the glass [37],[3].

Thermal tempering includes some limitations. These are:

-Not applicable to glasses under 2 mm

-Not suitable for complex-shaped glass materials

-It does not work on glasses with low thermal expansion coefficient.

The best method that can be applied to the glass materials mentioned above is chemical strengthening method. Chemical strengthening has advantages such as it can be applied to thin and complex shaped glasses with low thermal expansion coefficient, as well as providing higher strength and less optical distortion than thermal tempering.

4. Chemical Strengthening

Chemical strengthening involves immersing the glass sample in the molten alkali salt bath at a temperature below the glass transition temperature and replacing the smaller alkali ions in the glass sample with larger alkaline ions in the bath. It is a diffusion-controlled process. Typically, Na+ or Li+ is replaced by K+ and a compressive stress is created on the surface as a result of forcing a larger ion to be compressed into a "smaller" region (see Figure 2.7) [43].

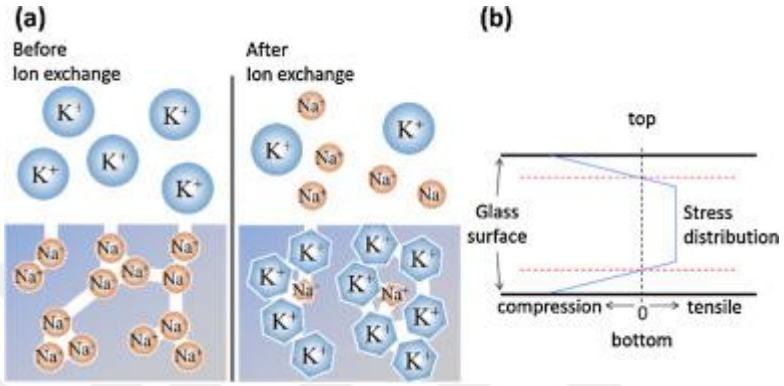


Figure 2.7 Mechanism of chemical strengthening process [44]

Since it is a diffusion-controlled process, the thickness of the compressive stress layer can be varied from a few microns to several hundred microns, depending on the glass composition, initial glass thickness, and the treatment schedule [1].

Ion exchange is based on the principle of exchanging ions in glass with different sized ions. When a smaller ion is replaced with a larger ion in a glass, the larger ion is literally squeezed into the surface, creating residual compressive stresses on the surface with a balancing tensile stress inside [36]. Residual compressive stress comparison between thermal tempering and chemical tempering is given in Figure 2.8.

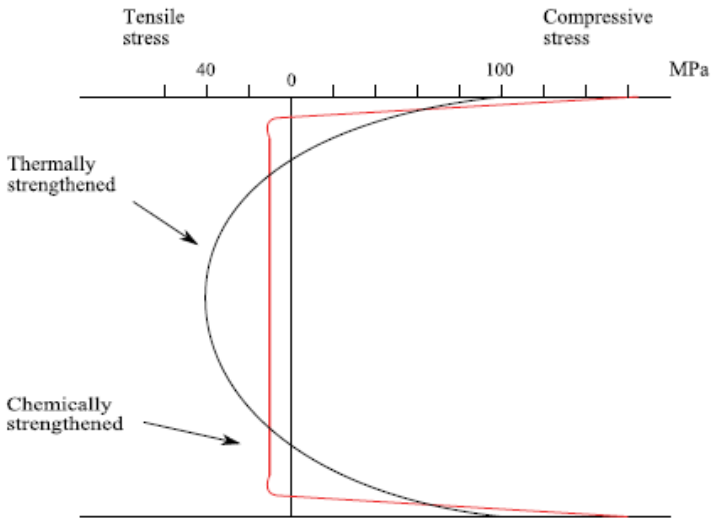


Figure 2.8 Comparison between the residual stress distributions in thermally and chemically strengthened glasses [1]

2.4 Chemical Strengthening

Chemical strengthening basically involves immersing the alkali-containing glass in an alkali-containing salt bath below the glass transition temperature, and the ion exchange process between the glass and the salt bath by the diffusion mechanism. Small alkali ions in the glass are replaced with larger alkali ions in the salt, thereby increasing the strength of the glass by creating a compressive stress on the surface.

Chemical strengthening was discovered in 1962 by Kistler and Acloque and Tochon. The initial excitement quickly declined after it was noticed that ordinary soda-lime glass products were slow to create a case depth of 25 mm, even after immersion for 4-24 hours. In recent years, the importance given to environmental concerns regarding product safety and the use of fossil fuel products has increased the interest in the process. Today, as an example of commercially successful glass products produced by chemical strengthening method; aircraft cockpit windshields, photocopier scanner glass, display windows in mobile personal electronic devices (e.g., mobile phones and MP3 players) and compact disks for portable hard drives can be shown [45].

Propagation of the microcrack on the surface is prevented by strengthening. Since the progress and growth of the crack requires the presence of tensile stress at the

crack tip, the formation of a compression layer in the area close to the surface prevents the crack growing. The crack does not grow unless the applied stress is large enough to exceed the compressive stress at the crack tip and does not generate tensile stress. In order to provide enough strength, the depth of the compression layer must be greater than the depth of the crack on the glass surface [46].

The general mechanism of the strengthening effect of the residual surface compression is shown in Figure 2.9 and Figure 2.10.

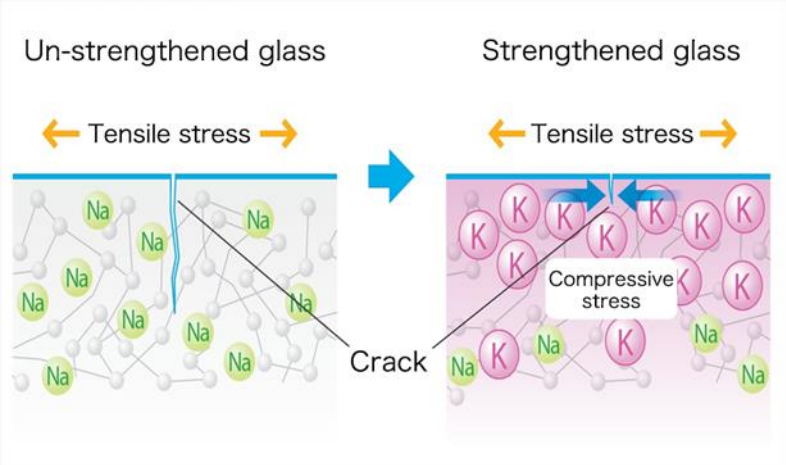


Figure 2.9 Crack progression of un-strengthened and strengthened glass [47]

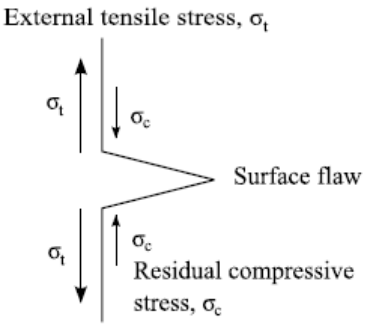


Figure 2.10 General mechanism of residual surface compression increasing the fracture strength. [20]

Since the chemical strengthening process is a diffusion-controlled phenomenon, the thickness of the compression layer depends on the glass composition, bath concentration, the thickness of initial glass and treatment schedule [1].

2.4.1 Ion Exchange

The principle of "ion exchange" was first described by Kistler (1962). Kistler et al. melted the soda-lime-silica glass in KNO_3 at temperatures below 350°C and observed that after a while there was a significant compressive stress up to 128,000 psi (~ 900 MPa) on the surface. This study was followed by a report in 1964 (Nordberg et al., 1964) for Na^+-K^+ ion exchange and its use for strengthening alkali-alumina-silica and alkali-zirconia-silica glasses. Since then, much of the literature on glass strengthening has been devoted to the ion exchange method [37].

Since the ion exchange temperature is below the transition point of the glass, there is no risk of surface deformation. Due to its change, there may be a change in the expansion coefficient of the surface glass, but this effect is relatively small [48]-[50]. Addition of any ion whose size is different from the original ion changes the structure of the material. This causes increased glass strength and thermal shock resistance and sealing of surface microcracks [8],[51].

The structure of the silicate glass consists of a continuous network of silicon-oxygen tetrahedral units interconnected at the corners. The bonds of the initial glass are very strong and highly oriented. In multicomponent silicate glasses, some cations can substitute silicon, or some can be embedded in the silicon-oxygen network. For example, the addition of alkali and alkaline earth elements (network modifiers) disrupts the continuous network, causing a decrease in glass viscosity [2],[3],[52]. These monovalent and divalent ions are embedded in the strong elastic Si-O network, and according to Kistler [9] they cause mechanical weaknesses. These mechanical weaknesses are particularly related to monovalent ions such as alkaline ions and provide internal movement due to the effect of diffusion or electrical potential. However, the Si-O network can be considered relatively stable during all diffusion processes (below glass transition temperature) due to strong and highly directed bonds. In such a network, some oxygens bind to two silicon ions and some to one. Network modifiers are distributed throughout the glass and therefore the glass structure can be considered as a solid texture of structural units that allow movement of mobile elements such as alkaline ions; consequently, the transfer of alkali ions can be described by heat conduction in solids with similar principles. As

a result, especially monovalent cations exhibit pronounced mobility in silicate glasses. This enables highly effective ion exchange processes [6],[20],[53].

Ion exchange in silicate glasses occurs when a glass containing a mobile ion, A, is exposed to another source of mobile ion, B, and the activation energy for the reaction is exceeded by thermal conditions. Ions in glass diffuse from glass to salt, while ions in salt diffuse into glass, which can be described in Eq. 2.4. The process is a mass transfer driven by concentration gradients. The source is typically a salt bath with good contact at the interface, i.e. a molten salt [6].

$$\overline{A}_{glass} + B_{salt} \rightleftarrows \overline{B}_{glass} + A_{salt} \tag{2.4}$$

When looking specifically for soda lime silicate glass; there is a network of silicon dioxide molecules in the core of a soda-lime glass. Among them, calcium and sodium ions are embedded. In the soda lime silicate glass, the surface compression layer is formed by the replacement of Na^+ with K^+ ions at a temperature lower than the glass transition temperature, at a specified time. The interstitial areas undergo elastic and plastic expansion, resulting in a wide surface compression and internal stabilization stress according to the elastic compatibility criteria [41],[54].

Ion exchange in silicate glasses has been known since 1913 [55] and has been previously attempted to chemically strengthen the glass surface [56]. To date, it has been studied to manufacture passive and active optical waveguides, production stress modulating systems, control the microstructural properties of glasses and better understand the environment-glass interaction mechanisms [57].

2.4.2 Diffusion Mechanism

Diffusion is a transport process in which molecules, atoms or ions are transported from one part of the system to another part as a result of the random movements of gases, liquids, or solid form species. Diffusion operates to increase entropy in the system and bring the system into an equilibrium state. Diffusion can be defined mathematically according to the same physical principles as heat conduction derived by Fourier in 1822 [15]. The similarity between heat conduction and diffusion was discovered in 1855 by Fick [58]. Basic definition of diffusion is given by Fick's First Law, Eq (2.5).

$$J = -D\frac{\partial C}{\partial x}\text{ , Fick's First Law} \quad (2.5)$$

J: Diffusion rate, flux (g/cm^{2}s)

D: Diffusion coefficient (cm^2/s).

C: Concentration (g/cm^3)

x: Diffusion distance (cm)

It refers that the concentration of other components, temperature and pressure are constant in space and time, and the diffusion medium is isotropic. $\partial C/\partial x$ is a concentration gradient and is a time independent value. This means that the difference in concentration between the less dense region and the denser region at each unit distance in the region where the diffusion takes place does not change over time. The value of ''D'' indicates how much the molecule can exceed the area in its medium per unit time, or its ability to move away from the medium. The "-" sign in the equation indicates that the molecular motion is towards the less dense region, the concentration decreases as it moves away from the dense region and therefore the flux value will always be "+". The ''D'' value of a molecule is not constant, it varies depending on the temperature, pressure and the properties of the medium in which the molecule moves (diffuses). When working under 1 atm pressure, it is assumed that the pressure variable does not affect the ''D'' value. Consequently, since ''D'' value is a value that can change according to temperature or ambient viscosity, it is specified as a diffusion coefficient, not as a diffusion constant [20].

Diffusion coefficient depends on temperature and Equation (2.6) is the diffusion adapted version of the Arrhenius equation, originally defined by Dushman and Langmuir in 1889 [59].

$$D = D_o e^{\left(\frac{Ea}{RT}\right)}\text{, Arrhenius Equation} \quad (2.6)$$

D_o: Constant, not temperature dependent

Ea: Activation energy (J/mol).

R: Ideal gas constant (J/Kmol).

T: Temperature (K).

Alkaline ion exchange in a glass is a diffusion-controlled reaction. In binary ion exchange, the diffuser A and B types are loaded and tend to diffuse at different rates in general. It is necessary to define an interdiffusion coefficient (mutual diffusivity), $\overline{D}$. Jost used flux gradient balance and described mutual diffusivity $\overline{D}$, which is a function of the two self-diffusion coefficients and the local ionic fraction (number of ions in a small volume) (N) of each species, and the self-diffusion coefficients (diffusivity) of each ions, D_1, D_2. Mutual diffusivity for a binary exchange, $\overline{D}$, can be written as follows:

$$\overline{D} = \frac{D_1 D_2}{N_1 D_1 + N_2 D_2} \tag{2.7}$$

Self-diffusion coefficient of ionic species in glass depends on many parameters, the two main parameters are ionic radius and valency [60]. In general, smaller ionic radius and lower valency allow for faster diffusion. During ion exchange, Na^+–K^+ interdiffusion coefficients in soda lime glasses were found to be almost constant and independent of local concentration and exchange time [1],[6],[20].

Interdiffusion is a function of the ratio of mobile ions involved in ion exchange. Therefore, in a typical concentration profile produced by ion exchange, mutual diffusivity is also a function of distance from the surface. This important parameter in the ion exchange process corresponds to the depth at which the ion exchange process takes place. The greater the depth, the more effective the surface strengthening process. Based on Fick's second law, the depth of ion exchange depends on the square root of time, as in Equation 2.8.

$$x = \sqrt{C\ t} \tag{2.8}$$

x is diffusion distance, depth of layer

C is a constant parameter which includes the diffusion coefficient,

t is the time required to reach x [6],[36].

In the current understanding of ion exchange kinetics, diffusion coefficient is managed by many different parameters such as salt bath composition, glass composition, change of ion types, temperature, pressure, etc [53]. Since an ion

cannot move to a new position until the ion in front of it comes out, the mobility of one ion must be strongly depends on other ions in the glass. Therefore, both the composition of the glass and the foreign alkali ions inserted into the structure of this glass affect the diffusion rate. If a glass sample is placed in a mixture of monovalent metallic ions, the diffusion of one of these ion types must depend on other ions available. A type of ion always diffuses preferentially.

The diffusion rate is also affected by temperature; however, there are restrictions on the temperatures that can be used. The temperatures used must be below the annealing temperatures of the base glass. If the temperature reaches the annealing point, the forces will be relieved almost immediately by reordering the network structure [13].

As a result, the reverse movement of sodium ions to the surface and potassium ions to the glass is controlled by diffusion and can be mathematically defined by Fick's first and second laws. The driving force for diffusion of both ion types are concentration gradients. The temperature of the molten salt provides the energy required to overcome any additional energy barriers in ion transport. Since the electrical neutrality must be maintained inside the glass, the diffusion rate of ions from the glass must be equal to the diffusion rate to the glass. Thus, the ion exchange process is controlled by the slowing of the counter diffusion ions [36].

2.4.3 Stress Generation

The potassium ion occupies a much larger (about 2.5 times larger) volume than the sodium ion, if some of the sodium ions in the soda-lime glass are replaced by potassium, a noticeable expansion occurs. In this case, exposure of a soda-lime glass to a melt potassium salt at a temperature at which diffusion can occur is expected to produce enormous stresses between the surface of the glass and the interior.

The science of stress production in glass during ion exchange is described by Cooper and Krohn [61] in a similar way to thermal stresses. For a semi-infinite (in y- and z-dimensions) glass plate of a thickness of 2 L being penetrated from the 7x-direction, the stresses at a location x are given by;

$$(\sigma_{xx}) = 0 \ , \ (\sigma_{zz})_x = (\sigma_{yy})_x = -\frac{BEC_x}{(1-v)} + \frac{1}{L}\int_0^L \frac{BEC_x}{(1-v)}dx \qquad (2.9)$$

where E is the Young's modulus; v is the Poisson's rate; and B=(1/3V) (∂V/∂C) linear network dilation coefficient (referred to as "'Cooper coefficient "in honor of late Alfred R. Cooper). Like the linear thermal expansion coefficient, the linear network dilatation coefficient is 1/3 of the relative change in volume V per unit change of the C concentration. Basically, stress is achieved by replacing the temperature (T) with concentration (C) and the linear thermal expansion coefficient a by the linear network dilatation coefficient B in all of the thermal stress equations [45].

2.4.4 Stress Relaxation

Stress production is closely related to the kinetics of interdiffusion and the difference between the size of exchanging ions. Although the diffusion rates increase exponentially with temperature, the stress rate that occurs as the change temperature approaches the glass transition temperature decreases with stress relaxation. That means high temperatures, in which ion exchange is applied, naturally accelerate glass transitions such as stress and structural relaxation and cause compressive stress reduction. Stress relaxation has a very critical effect on chemical tempering. Stress relaxation has been studied extensively as it explains stress profiles anomalies. The stress profile is affected by this stress release or relaxation due to viscous flow or thermal history of glass [6].

Varshneya suggests that ion exchange above or near glass transition temperature results in very little strengthening effect depending on time. Varshneya published studies on network relaxation and concluded that:

I: elastic deformation occurs when a smaller ion is replaced with a larger ion and

II: Plastic deformation occurs by re-adjusting non-bridged oxygen or displacement and bond bending of bridged oxygen [62]. These structural changes, such as changing the distances between bridging/non-bridging oxygen and potassium, reduce the accumulated stress. Structural changes that can occur by breaking and reshaping the bridging oxygen, may lead to further stress loss. Stress relaxation,

perhaps due to such processes and viscous flow, explains stress reduction or in extreme cases to produce a stress-free ion exchange glass. It should be noted that the structural evolution and stress relaxation of glass during ion exchange and chemical strengthening are open questions and should be answered [6].

The establishment of surface compression is the net result of two competing processes, ion exchange and viscous relaxation [63]. Stress relaxation rate increases with increasing surface modification depths. Therefore, it appears that the relaxation rate depends not only on the concentration of exchanged ions in the glass, but also on the overall relaxation history of the glass [64]. Burggraaf & Cornelissen explained this in terms of alumina coordination and its effect on non-bridging oxygen [65].

For successful chemical strengthening, a strong compressive stress with a sufficient depth is required to strengthening surface flaws and ultimately increase mechanical strength. Due to the diffusional nature of the process, the production of the desired exchanged layer requires several hours to be subjected to high temperatures. Therefore, finding critical parameters and effects are the first requirements for chemically strengthening of glass. Temperature and time should be chosen at intervals that will not cause excessive stress relaxation [6]. The optimum temperature is about 90 K below glass transition temperature [66].

2.5 Corrosion of Glass

It is important to know the physical and chemical properties of the glass surface in order to understand the glass corrosion process. The coordination of the atoms in the glass mass structure and the coordination of the atoms on the glass surface are different. This difference causes chemical bonds on the surface to be more prone to chemical reactions. The processes applied to the glass surface or the environment the glass surface is exposed to may cause some components to move away from the glass surface, the reaction of water, moisture, dew and gases such as CO_2 and SO_2 in the atmosphere with the atoms on the glass surface or physical or chemical adsorption to the glass surface. All this can change the chemical composition of the glass surface or the surface topography. As a result, the chemical behavior of the glass surface changes. Investigation of glass surface properties, namely

characterization of the glass surface and sub-surface composition and surface topography down to the nanometer level is the first important step to understand the corrosion process and improve the glass surface. Glass corrosion occurs in two stages. The 1st stage corrosion reaction is the formation of Si–OH groups as a result of the ion-displacement reaction and the removal of the network regulators from the glass structure. The second stage corrosion reaction is the breakdown of the silica network when pH > 9.

1st stage corrosion reaction: When the glass surface is exposed to water, moisture, dew, the ion that occurs between the network regulators such as Na^+, K^+ (alkali ions) and Ca^{2+}, Mg^{2+} (alkaline earth ions) and H^+ ions of the water Si–OH groups are formed as a result of displacement reaction and the network regulators go out of the glass structure [67]-[71]. The reactions are as follows:

$$(\equiv Si{-}O^{-}Na^{+})_{glass} + H_2O \rightarrow (\equiv Si{-}OH^{-})_{glass} + Na^{+}OH^{-} \quad (2.10)$$

$$(\equiv Si{-}O^{-}\ Ca^{2+}\ {-}O^{-}Si\equiv)_{glass} + 2H_2O \rightarrow 2(\equiv Si{-}OH^{-})_{glass} + Ca^{2+} + 2OH^{-} \quad (2.11)$$

As a result of these reactions, a hydrated glass surface that is poor (leached) in terms of alkali and alkaline earth ions occurs. Depending on the chemical composition of the glass, the leaching process gradually slows down and stops at a certain stage. Network components remain unchanged at this stage.

2nd stage corrosion reaction: As the ion-displacement reaction progresses, the pH of the glass surface or the aqueous solution in contact with the surface may rise above 9. In this case, the leaching speed decreases, and the hydroxyl (OH^-) ions attack the Si–O–Si bonds of the network. This reaction dissolves the glass components, network structure of silica is broken down [67]-[71]. The reaction is as follows:

$$(\equiv Si{-}O{-}Si\equiv)_{glass} + OH^{-} \rightarrow (\equiv Si{-}OH^{-})_{glass} + {-}O{-}Si\equiv \quad (2.12)$$

A schematic representation of the corrosion mechanism of glass is given in Figure 2.11.

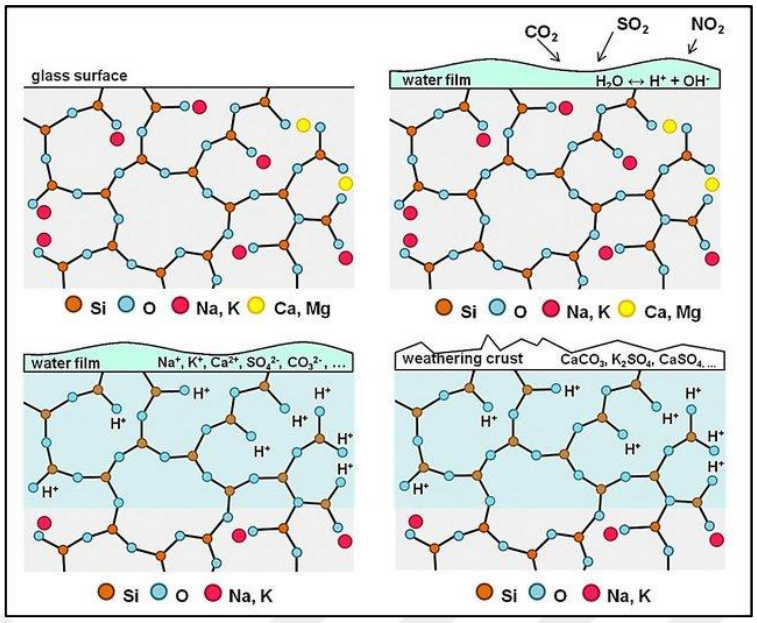


Figure 2.11 Glass corrosion mechanism a) (weathering) starts with a clean and uncorroded surface. (b) The formation of a water film occurs, due to the atmospheric conditions, allowing ionic exchange between the ions H^+ and H_3O^+ of water and the alkaline ions present in glass, which may be reinforced by the presence of acid gases. (c) This lixiviation reaction starts slowly but accelerates overtime; after the formation of a hydrated layer (light blue in the figure), rich in silica and alkaline oxides, (d) the glass surface becomes more resistant to the attack of water and the surface pH increases. The crystalline corrosion products (salts) stay in the glass surface after the water evaporates [72]

As a result of these reactions, visible defects such as clouding, or staining occur on the corroded glass surface.

Fourier Transform Infrared Spectroscopy (FTIR) is one of the important techniques used for this purpose. Studies on glass corrosion characterization using IR spectroscopy technique started in the 70's. This technique is a very useful technique used to monitor the glass corrosion process and to assess the degree of corrosion. As an example, the IR reflectance spectra of a glass sample subjected to accelerated corrosion test by Ethridge [73] are given in Figure 2.12. In the IR spectrum of newly produced glass, there is a peak observed at 1060 cm^{-1} wavelength of Si-O-Si bond vibration. As the corrosion process progresses, it is seen that this peak shifts to the

left, i.e., towards the region with higher wave number, and starts to shoulder at 960 cm^{-1} at the end of the 4th hour and appears in the spectrum as the second peak at the end of the 16th hour. This peak observed at 960 cm^{-1} belongs to the $Si–O^-$ non-bridging oxygen (NBO) bond vibration. This result shows that the silica network structure is disintegrated, that is, the 2nd stage corrosion reaction has taken place.

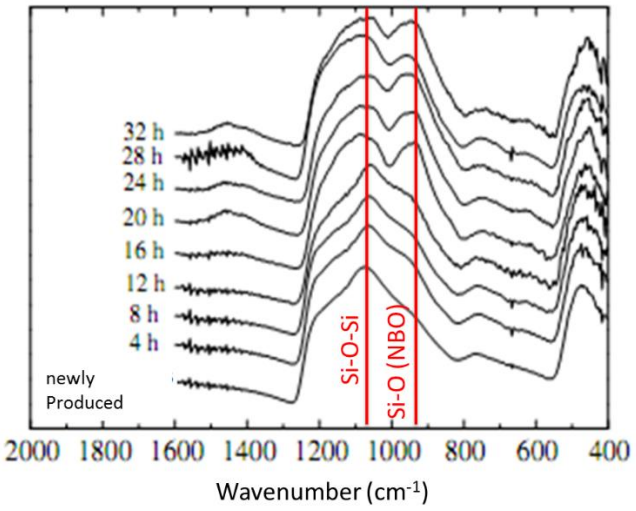


Figure 2.12 The IR spectra of glass samples subjected to fastened corrosion test [73]

In the study conducted by Gösterişlioğlu et al. [74], the corrosion behavior of chemically tempered glasses of different compositions was investigated.

3
Experimental Studies

In this dissertation study, the effect of salt baths contaminated with different calcium compounds on chemical tempering efficiency of commercial soda-lime silicate glasses is evaluated in terms of mechanical, structural, and optical properties. In addition, corrosion behavior of glass samples was investigated after chemical tempering process by applying structural and optical tests. All the results are compared with samples chemically tempered in pure KNO_3 salt bath. Furthermore, chemical analysis of salt baths was carried out in order to investigate the effect of different calcium impurities on salt bath.

3.1 Sample Preparation

1.1 mm thick soda-lime silicate float glass plates of 30 x 30 cm in size received from Trakya Cam Sanayii A.Ş. were cut from tin sides into square samples of 5 x 5 cm in size with a CO_2 laser cutting device. The elemental composition of glasses were determined using a Rigaku Primus II X-Ray Fluorescence (XRF) spectrometer (see Table 3.1).

Table 3.1 Chemical composition of glasses

Soda-lime silicate (SLS) glass	**SiO_2**	**Na_2O**	**CaO**	**MgO**	**K_2O**	**Al_2O_3**
Composition (wt%)	72	13	9	4	1	1

Pre-cut glass samples were then cleaned in an ultrasonic bath at 40 °C using distilled water and alcohol, respectively for 2 minutes and then dried with pressured nitrogen gas flow. The dried samples were placed in specially designed baskets made of 316 grade stainless steel for chemical tempering process (see Figure 3.1).

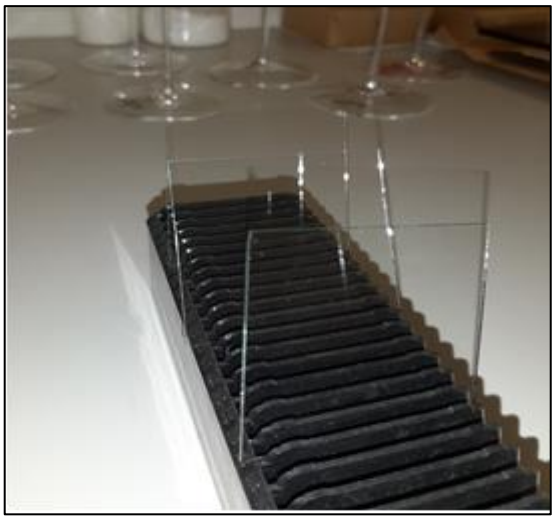


Figure 3.1 Image of pre-cut samples ready for chemical tempering

3.2 Chemical Tempering Process

For chemical tempering process, boxes made out of 316 grade stainless steel were filled with KNO_3 salt (Quality Chemicals, 99.9% purity) and placed in a Protherm CWF 1300 furnace. Afterwards, stainless steel baskets containing glass samples were immersed in molten salt baths and subjected to chemical tempering at 450 °C for 4 hours (see Figure 3.2). These tempering conditions were chosen according to our prior experience for obtaining maximum mechanical performance without relaxation. As a result of the tempering process, glass samples were cleaned with distilled water in order to remove the salt residues and then dried with nitrogen.



Figure 3.2 Chemical tempering set-up (left: stainless steel basket containing glass samples, right: stainless steel box containing KNO_3 salt contaminated with different amounts of calcium compounds)

For chemical tempering process, salt baths were contaminated with Ca^{2+} impurities in different amounts by using different compound forms (see Table 3.2) The calcium contamination amounts were determined by considering the effect of these impurities on chemical tempering efficiency.

Table 3.2 Amount of different Ca^{2+} containing compounds used in experimental studies

$Ca(NO_3)_2$	**$CaCO_3$**	**CaO**
0	0	0
1.0	-	-
2.0	-	-
3.5	3.5	3.5
6.0	6.0	6.0
8.0	8.0	8.0
20.0	20.0	20.0

* All amounts are given in ppm of Ca^{2+} ion

3.3 Aging Process

Aging test was realized after chemical tempering process to examine the resistance of glass samples against atmospheric corrosion. Aging test was applied on 3 samples for each calcium contamination amount and compound form. The aging test was carried out by keeping the glass samples in Ascott-H450T CTG 060 brand humidity cabinet for 14 days, at 40 °C under 95% humidity. After 14 days, glass samples were taken out of the aging chamber, were washed with distilled water, and dried by nitrogen and thereby made ready for further tests and characterization studies.

3.4 Test and Characterization Studies

3.4.1 Surface Stress Characterization

The purpose of chemical tempering process is to increase the strength of glass sample by creating a compressive stress layer on the surface. Since the strength of the sample increases in direct proportion to this compressive stress layer (CS) formed on the surface and the depth of this layer (DOL), it is necessary to measure the surface compressive stress and depth of layer in order to determine the efficiency of the chemical tempering process. For this purpose, the CS and DOL values were measured on the sample surface using FSM-6000-LE model surface stress meter. In this method, by letting the light to propagate along the surface of the glass, the stress on surface and the depth of stress layer can be measured according to photo-elastic techniques. This machine is equipped with a computer, which can reduce the error of the measurer and facilitate the management of the measurement data. Analysis was carried out by taking measurements from three different points of three different tempered samples and the average of these values was taken.

3.4.2 Structural Analysis

Corrosion negatively affects the appearance, strength, chemical resistance, reactivity, and optical properties of the glass product. The characterization of glass corrosion is very important in understanding the degree and stage of corrosion. Fourier Transform Infrared Spectroscopy (FTIR) is one of the important techniques used for this purpose. This method is based on the principle of measuring the vibration or rotation frequencies of chemical bonds by absorption of the IR beam. In

infrared spectroscopy, the sample is irradiated with an electromagnetic wave containing all frequencies in the infrared region, and the transmitted or absorbed light is examined.

In this study, structural analysis was performed with a Bruker Hyperion 3000 model FTIR device in order to examine the changes caused by the chemical tempering process in the network structure of glass. In addition, in order to observe the change caused by the aging process in the bonding structure of the glass, this test was repeated after the aging process and the results were compared with each other.

3.4.3 Optical Analysis

For optical analysis, transmittance and haze tests were applied to examine the effects of different calcium-based salt bath impurities on the optical properties of glasses. Transmittance and haze tests were applied on 3 samples for each calcium contamination amount and compound form using BYK Haze-Gard-i model device.

3.4.4 Mechanical Analysis

For mechanical analysis of glass samples ring-on ring tests and Vickers hardness measurements were applied.

The ring-on-ring test is a standardized test for strength measurements on brittle materials such as glasses and ceramics. Mechanical defects determine the strength of materials in these tests. The ring-on-ring test involves the creation of a uniform axially symmetrical stress condition in the middle of the sample surface of an annular plate. This is accomplished by placing the sample on a segmented circular ring and applying a load to its upper surface, which is transmitted through a circular ring that is concentric with the segmented support and of a smaller diameter. This test is a biaxial test and measures the strength of a glass or ceramic surface in both width and length direction.

In this study, ring-on-ring tests were applied in order to determine the fracture mechanics of glass samples chemically tempered in contaminated salt baths containing different Ca^{2+} impurities. 14 samples of 5 x 5 cm in size were tested with an Instron 3366 model device at a speed of 1.3 mm/min. As a result of the test, the average breaking loads were determined.

Weibull distribution was used to determine the reliability of the measurement, which relates the fracture load (N) to the failure probability. The Weibull modulus is a dimensionless parameter of the Weibull distribution that is used to describe the variability in mechanical strength of brittle materials such as glass. This model can provide accurate estimates of the expected average and standard deviation of glass strength. The Weibull distribution can be calculated by the function given in Equation 3.1.

$$P_f(\sigma) = 1 - e^{\left\{-\left(\frac{\sigma}{\sigma_n}\right)^m\right\}} \tag{3.1}$$

where $P_f(\sigma)$ is the cumulative failure probability, σ_n is the nominal strength, and m is the shape parameter (Weibull modulus). [75]

To easily access the information, a linearized version of the equation was used, as given in Equation 3.2. [76]

$$\ln\left(-ln\left[1-P_f(\sigma)\right]\right) = m.\ln(\sigma) - m.\ln(\sigma_n) \tag{3.2}$$

Hardness is a relative measurement, and it is a measure of the resistance of materials against abrasion, scratching, puncture, that is, the resistance of the materials against plastic deformation. Due to its simplicity, one of the most common mechanical tests on the material is the hardness test. There is also a parallel relationship between the hardness of material and other mechanical properties, so that some other properties can be obtained. Vickers hardness measurement method consists of applying pressure to the surface of the piece of material whose hardness is to be measured, under a certain load of a pyramid shaped tip with a square base for a certain period of time and measuring the trace diagonals that occur after the load is removed. The Vickers hardness value is the division of the test load expressed in kg by the area of the trace expressed in mm^2. Printing is applied to the glass with a diamond square pyramid with a peak angle of 136° (see Figure 3.3).

In experimental studies, the hardness measurements were carried out by applying a 50 g load on the sample surface for 10 seconds using DHV-1000(Z) Micro Vickers Hardness Tester. Five indentations made for each sample and mean values were used. After the experiment, it is necessary to measure the square-shaped trace

diagonals precisely to find the correct Vickers hardness value. This measurement was made with a metallurgical microscope attached to the instrument. The trace image created on the sample was then transferred to the measuring screen. The lengths of the diagonals were precisely measured and averaged separately with the help of two moving rulers on the measurement screen.

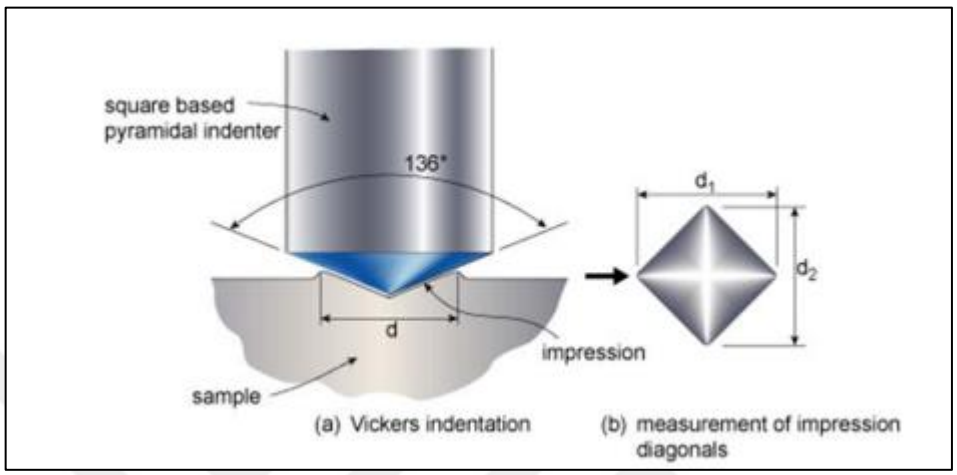


Figure 3.3 Schematic representation of the Vickers indentation technique [77]

The Equation 3.3 was used to determine the Vickers hardness value.

$$Vickers\ hardness = 1.8544\,.\frac{F}{d^2} \tag{3.3}$$

where F is the applied load,

$d = \frac{(d_1+d_2)}{2}$ d_1, d_2 are measured diagonal lengths.

In addition, the Vickers indentation technique was used to examine the crack resistance of samples. In this context, the load applied to the sample was increased in a controlled manner and crack formation load was examined. Load values applied to the samples to examine the crack behavior were 100, 200, 300, 500, and 1000 g, respectively.

3.4.5 Methylene Blue Test

The methylene blue test was applied to clearly identify the corrosion of glass samples. If corrosion has occurred on the glass surface, these corrosion spots can be clarified with methylene blue solution. In experimental studies, glass samples were

immersed and removed from the beaker in which some methylene blue solution had been placed so that all sides touch the methylene blue solution. If there is corrosion, methylene blue will enter the corrosion pits and blue stains will appear on the glass surface.

3.4.6 pH Measurements

Since glasses are exposed to salt bath for a long time during chemical tempering process, analysis of the salt pH is quite important. Basic salts with high pH cause corrosion on the surface of the glass by disrupting the Si–O–Si network structure. Therefore, pH measurements were realized in order to determine the corrosion behavior of chemical tempering salts by examining the change in acidity-basicity degree as a result of different Ca^{2+} containing compounds added. For pH measurements, aqueous solutions containing 5% salt were prepared in 100 ml beakers and the results were recorded by using a pH-meter.

3.4.7 Alkalinity Tests

Alkalinity analysis, that is related to the pH of the chemical tempering salts, was applied to evaluate the corrosion behavior which could be caused by carbonate, bicarbonate and hydroxide ions in the salt solution. Alkalinity is basically a measure of the acid neutralization capacity of water, in other words, the amount of acid required to lower the pH to 4.3 and is defined as the quantitative capacity of water to react with strong acids up to a specified pH value. The measured alkalinity value varies depending on the final pH value. High alkalinity means high pH. Since alkalinity in surface waters is a function of carbonate, bicarbonate and hydroxide content, it is taken as a measure of the concentration of these components. Bicarbonate (HCO_3^-) has a pH between 4.3 and 8.3 and it is the most common alkalinity in natural water bodies. Carbonate (CO_3^{2-}) has a pH ranging from 8.3 to 10. When the pH value is greater than 10, it has hydroxide (OH^-) alkalinity.

In this study, alkalinity was determined from the amount of acid consumed in the titration of the samples with standard acid to a predetermined pH value. The type of alkalinity was determined by titration at room temperature using a pre-calibrated pH meter using phenolphthalein and methyl orange indicators. In this context,

firstly four drops of phenolphthalein were added to the prepared 10% salt-water solutions. If it contains hydroxide or carbonate gives pink color with phenolphthalein indicator, if there is acid it becomes colorless. If the solution turns pink, it is titrated with 0.02 N H_2SO_4 acid until it returns to its original color and the amount of acid consumed (P, Phenolphthalein alkalinity) is recorded. If there is no pink color, the pH of the water is less than 8.3 and the hydroxide and carbonate alkalinity is zero. After this process, four drops of methylorange indicator were added into the solution. The amount of acid consumed was recorded by titrating with H_2SO_4 until pH 4.3. This value is the turning point pH at which the color of the methylorange indicator changes and the solutions become acidic and is predetermined for alkalinity analysis. The endpoint pH is 4.3 because it is the equilibrium pH at the moment when bicarbonate ions are converted to carbonic acid. The methylorange indicator turns yellow when one of the three alkalinities is found in the water and turns red if there is acid. In the calculations that follow the titration, the types of alkalinity are found by distributing the amount of acid consumed with the indicators used according to the ions that make up the alkalinity. According to American literature, phenolphthalein alkalinity and methylorange alkalinity are indicated by the letters P and M, respectively.

P = Phenolphthalein Alkalinity (0.02 N H_2SO_4 consumption after phenolphthalein indicator addition (ml))

M = Methylorange Alkalinity (0.02 N H_2SO_4 consumption after phenolphthalein indicator addition (ml))

If P= 0, alkalinity only depends on bicarbonate (HCO_3^-).

If P = M, alkalinity only depends on hydroxide (OH^-).

If 2P = M, alkalinity only depends on (CO_3^{2-}).

If 2P > M, alkalinity depends on carbonate (CO_3^{2-}) and hydroxide (OH^-).

If 2P < M, alkalinity depends on carbonate (CO_3^{2-}) and bicarbonate (HCO_3^-).

4
RESULTS AND DISCUSSION

In this thesis study 1.1 mm thick soda-lime silicate flat thin glasses were chemically tempered in KNO_3 salt baths contaminated with different calcium compounds and then subjected to aging process. The effect of calcium contamination of the salt baths on chemical tempering efficiency was studied in terms of mechanical, structural and optical properties. In addition, pH measurement and alkalinity analysis were performed to evaluate the acidity of salt baths used in chemical tempering.

In experimental studies, four different salt baths were studied, and the results of the experiments were collected under four main headings considering the composition of the salt baths. The salt baths used were named as follows:

1. Pure KNO_3 Salt Bath (used as a reference)
2. $Ca(NO_3)_2$ Contaminated KNO_3 Salt Bath
3. $CaCO_3$ Contaminated KNO_3 Salt Bath
4. CaO Contaminated KNO_3 Salt Bath

4.1 Results for Pure KNO_3 Salt Bath

4.1.1 Compressive Stress and Depth of Layer Analysis Results

The surface compressive stress (CS) and depth of layer (DOL) analysis results for glass samples chemically tempered in pure KNO_3 salt bath were detected as 556 MPa and 9.6 μm, respectively.

4.1.2 Vickers Hardness Test Results

The average hardness value for chemically tempered glasses in pure KNO_3 salt was determined as 617.5 HV.

4.1.3 Ring on Ring Test Results

The average breaking load resulting from the ring-on-ring test was obtained as 1910 N for chemically tempered glasses in pure KNO_3 salt.

4.1.4 Structural Analysis Results

FTIR analysis was performed before and after aging process for glasses tempered in pure KNO_3 salt bath, and the resultant spectra are given in Figure 4.1. As can be seen from the FTIR spectra, there is no significant difference in the band structure for original and tempered glasses before and after aging process. Asymmetric vibrations of Si–O–Si bonds and Si–O (NBO) bond vibrations were determined for both original and tempered samples before and after aging. Although after aging process there was a slight shift to lower wavenumber (to the right) in the peak corresponding to Si–O–Si bonds, it was observed that there was no shoulder displacement in the band position representing the vibration of Si–O non-bridging oxygen bonds. This shows that there is no significant corrosion on the glass surface.

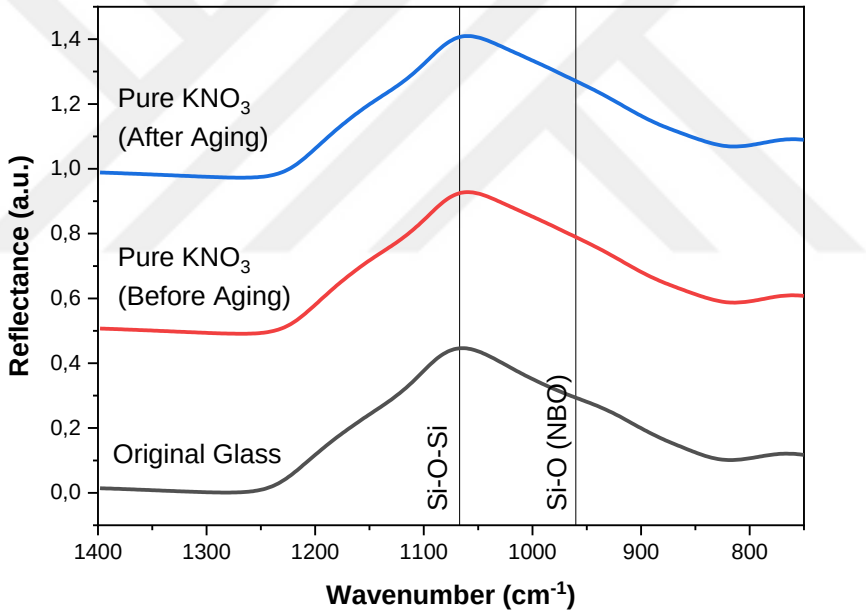


Figure 4.1 FTIR spectra of original glass and chemically tempered glass in pure KNO_3 salt bath before and after aging process

4.1.5 Macro Examination Results

The macro photograph of chemically tempered glass in pure KNO_3 salt bath after aging process is given in Figure 4.2. The photo clearly shows that there is not a significant corrosion to create deterioration on the glass surface.

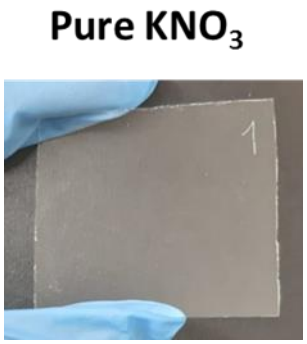


Figure 4.2 Macro photo of aged glass chemically tempered in pure KNO_3 salt bath

The macro photograph taken as a result of the methylene blue test is given in Figure 4.3. Since there is no obvious staining on the sample surface after aging, it is understood that corrosion has no detectable effect on the glass surface in macro scale.

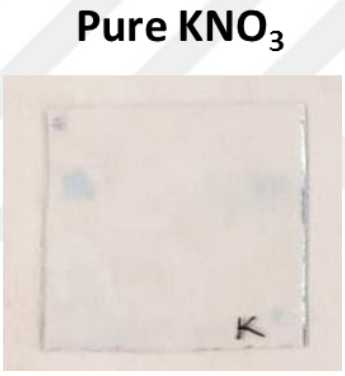


Figure 4.3 Macro photo of aged glass chemically tempered in pure KNO_3 salt bath after methylene blue test

4.1.6 Optical Analysis Results

Transmittance and haze analysis results of chemically tempered glass in pure KNO_3 salt bath before and after aging process are given in Table 4.1. As can be seen from the results, there is no significant change in transmittance and haze values before and after aging process.

Table 4.5 Transmittance and haze test results of glass sample chemically tempered in pure KNO_3 salt bath

Sample	Transmittance (%)		Haze (%)	
	Before Aging	After Aging	Before Aging	After Aging
Original glass	91.1	91.1	0.10	0.20
Chemically tempered glass in pure KNO_3	91.0	91.0	0.14	0.16

4.1.7 pH and Alkalinity Analysis Results

pH and alkalinity values of pure KNO_3 salt bath were measured after tempering process and the obtained values are given in Table 4.2. It was determined that the pH value was within acidic limits (5.67), while the alkalinity depends only on bicarbonate and not on carbonate and hydroxide alkalinity.

Table 4.2 pH and alkalinity results of pure KNO_3 salt bath

	Bicarbonate Alkalinity (HCO_3^- mg/L)	Carbonate Alkalinity (CO_3^- mg/L)	Hydroxide Alkalinity (OH^- mg/L)	pH
Pure KNO_3 bath	4.80	–	–	5.67

4.2 Results for $Ca(NO_3)_2$ Contaminated KNO_3 Salt Bath

4.2.1 Compressive Stress and Depth of Layer Analysis Results

The results of surface compressive stress and depth of layer analysis of glass samples chemically tempered in $Ca(NO_3)_2$ added salts are given in Figure 4.4. With the addition of $Ca(NO_3)_2$, the surface compressive stress and the depth of compressive stress layer values first showed a slight decrease compared to pure KNO_3 salt. With increasing amount of $Ca(NO_3)_2$ contamination, the surface

compression values gradually decreased, while at 20 ppm contamination amount this value became too low to be measured. However, with increasing $Ca(NO_3)_2$ contamination there was no significant change in the depth of layer. This shows that the $Ca(NO_3)_2$ contamination limited the ion exchange, and after a certain amount (20 ppm), it had a blocking effect by completely preventing the K^+-Na^+ ion exchange. Depth of layer, which is an indicator of how deep ions move from the surface to the sample, showed a slight decrease when the $Ca(NO_3)_2$ contamination was first included, however did not show a significant change with increasing amount of $Ca(NO_3)_2$. In other words, although $Ca(NO_3)_2$ limited K^+-Na^+ ion exchange and prevented it after a certain amount, it did not affect the diffusion process of the displaced ions from the sample surface to the interior. However, with the addition of 20 ppm of $Ca(NO_3)_2$, this value fell below 5 µm, therefore it could not be properly detected.

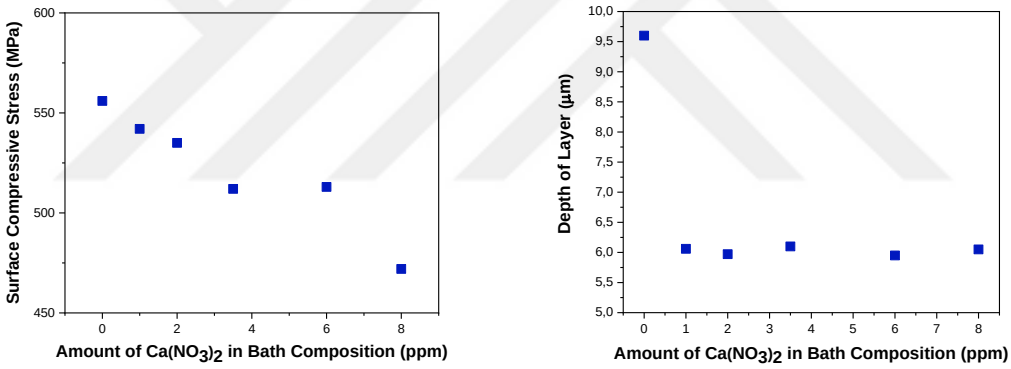


Figure 4.4 Variation of CS and DOL values for glasses tempered in different amounts of $Ca(NO_3)_2$ contaminated KNO_3 salt bath

4.2.2 Vickers Hardness Test Results

Vickers hardness test results of glass samples chemically tempered in different amounts of $Ca(NO_3)_2$ added salts are given in Figure 4.5. Addition of 1 ppm of $Ca(NO_3)_2$ to the salt bath initially increased the hardness value, however further increment of $Ca(NO_3)_2$ addition caused a steady decrease in the hardness values.

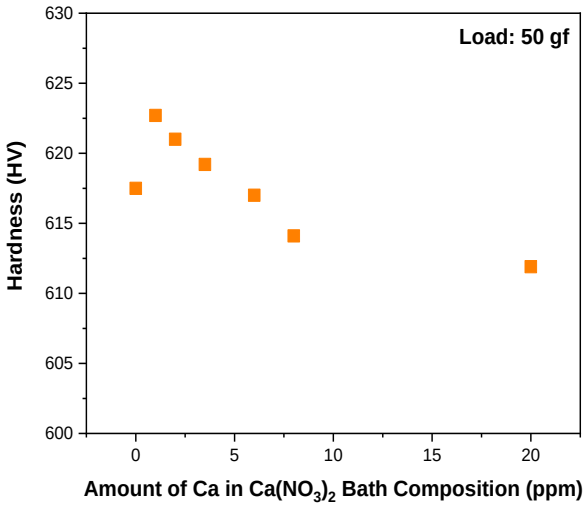
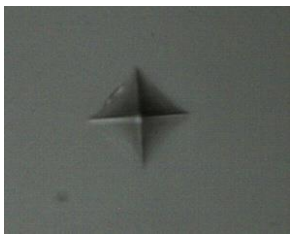
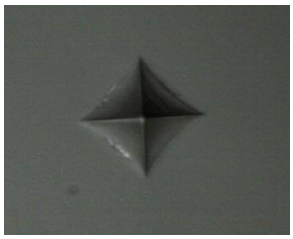
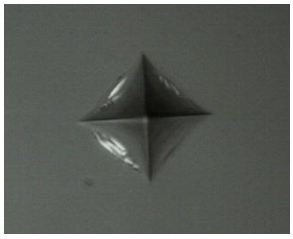
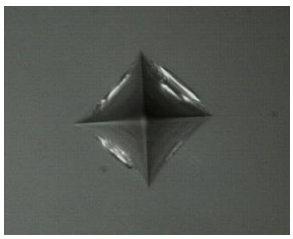
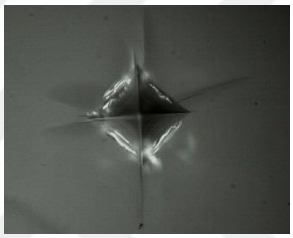


Figure 4.5 Vickers hardness test results of glass samples chemically tempered in different amounts of $Ca(NO_3)_2$ containing salts

Table 4.3 shows the crack formation behavior of glass sample chemically tempered in 8 ppm $Ca(NO_3)_2$ contaminated salt bath under 100, 200, 300, 500 and 1000 g loads.

Table 4.3 Crack formation behavior of glass sample chemically tempered in 8 ppm $Ca(NO_3)_2$ contaminated salt bath

Load, g	Micrographs
100	
200	

300	
500	
1000	

4.2.3 Ring-on-Ring Test Results

For ring-on-ring tests, glass samples chemically tempered in 8 ppm $Ca(NO_3)_2$ contaminated salt bath was selected to examine the fracture mechanics and the average load value at the moment of break was measured as 1288 N. Compared to the average breaking load value (1910 N) of glass samples chemically tempered in pure KNO_3 salt bath, the average breaking load value of glass samples tempered in 8 ppm $Ca(NO_3)_2$ containing salt bath showed a significant decrease.

4.2.4 Structural Analysis Results

According to the FTIR spectroscopy results, it was observed that there is no significant change in the structure of glass samples before the aging process compared to the original and pure KNO_3-tempered glass (see Figure 4.6). After aging, it was observed that there was no significant change in the band structure up to 8 ppm $Ca(NO_3)_2$ amount, however after this amount of contamination structural

changes became visible. After aging, for glasses chemically tempered in 8 ppm $Ca(NO_3)_2$ contaminated bath it was observed that there is a slight shift to the lower wavenumbers (1056 cm^{-1}) in the peak representing the Si–O–Si vibrational band observed at 1060 cm^{-1} in original glass. The Si–O band related to NBO vibration and detected at 960 cm^{-1} in original glass showed a small shoulder after aging. Therefore, FTIR spectra reveal that glasses chemically tempered in 8 ppm $Ca(NO_3)_2$ contaminated bath shows slight corrosion after aging process possibly related to stage 1 corrosion.

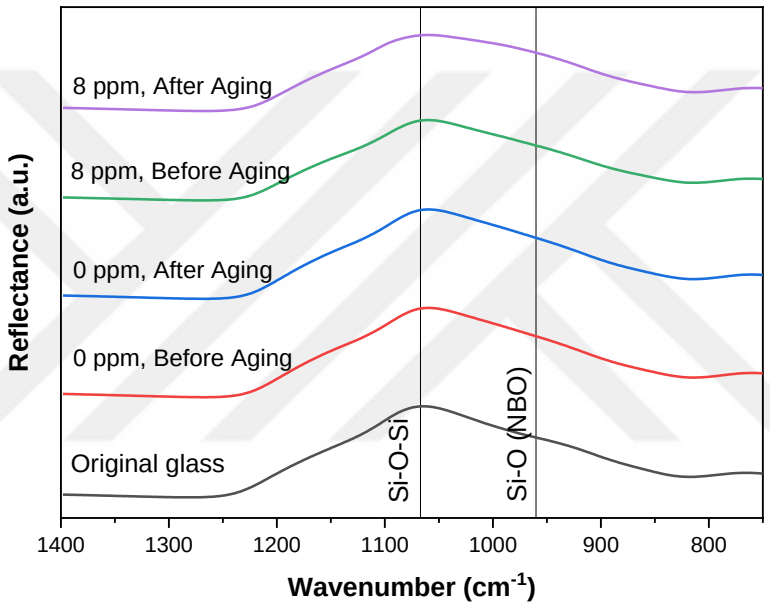


Figure 4.6 FTIR spectra of original glass and glasses chemically tempered in pure (0 ppm) and $Ca(NO_3)_2$ contaminated (8 ppm) KNO_3 salt bath before and after aging process

4.2.5 Macro Examination

The macro photographs of aged glass samples chemically tempered in different amounts of $Ca(NO_3)_2$ containing salt baths are given in Figure 4.7. Compared to the glass sample tempered in pure salt bath, increasing the amount of $Ca(NO_3)_2$ contamination in the tempering salt results a significant surface deterioration after the aging process.

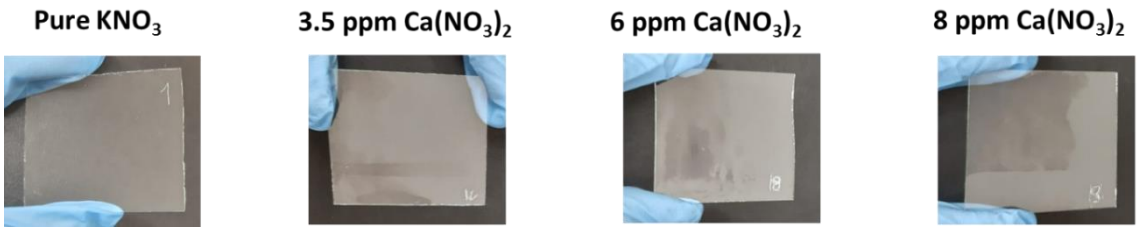


Figure 4.7 Macro photos of aged glass samples chemically tempered in different amounts of $Ca(NO_3)_2$ containing salt baths

The macro photographs taken as a result of the methylene blue test applied to make the corrosion on the sample surface clear after the aging process are given in Figure 4.8. As a result of the test, it was determined that the sample tempered with pure KNO_3 salt did not have a significant staining, but staining rose with the increase in the amount of $Ca(NO_3)_2$ in the salt bath.

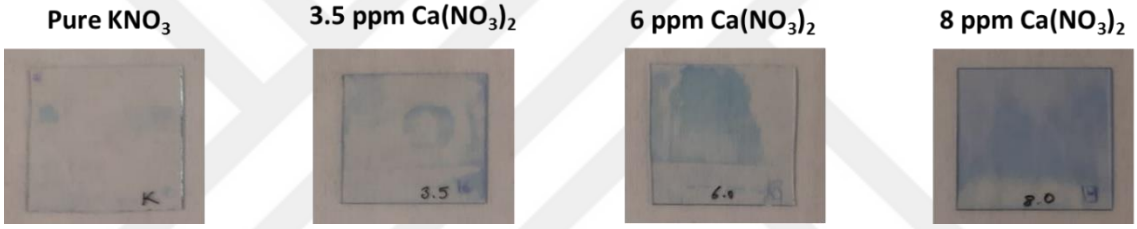


Figure 4.8 Macro photos of glass samples chemically tempered in different amounts of $Ca(NO_3)_2$ containing salt baths after methylene blue test

4.2.6 Optical Analysis Results

Transmittance and haze values before and after aging process for glass samples chemically tempered in salt baths having different amounts of $Ca(NO_3)_2$ are given in Figure 4.9. As can be clearly seen, changing amount of $Ca(NO_3)_2$ generally did not cause a significant change in haze and transmittance values before and after aging process.

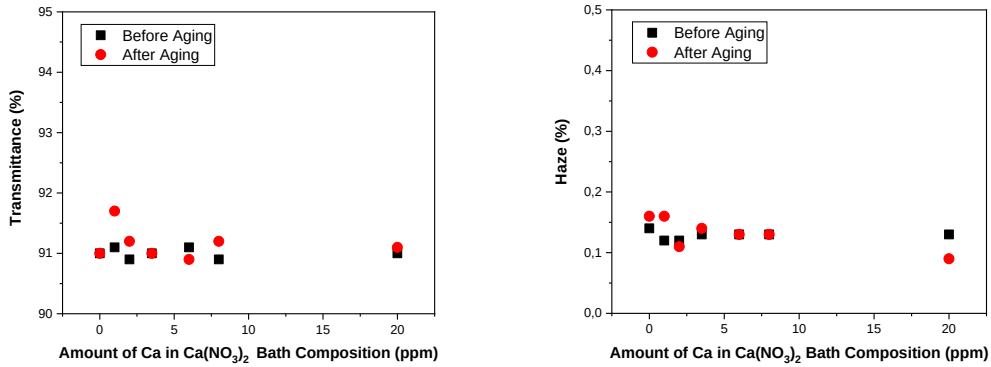


Figure 4.9 Transmittance and haze results of glasses chemically tempered in different amounts of $Ca(NO_3)_2$ contaminated salt baths

4.2.7 pH and Alkalinity Analysis Results

pH and alkalinity results for different amount of $Ca(NO_3)_2$ added salts are given in Table 4.4. Slight changes were observed in pH and alkalinity values with increasing $Ca(NO_3)_2$ content. Alkalinity was solely due to bicarbonate and not dependent on carbonate and hydroxide alkalinity. The pH values remained within acidic limits for all contamination amounts. These results show that the addition of $Ca(NO_3)_2$ does not significantly increase the pH and alkalinity of the salt and therefore does not create a corrosive environment that can significantly affect the surface of the glass.

Table 4.4 pH and alkalinity test results for different amount of $Ca(NO_3)_2$ added salts

Bath Composition [$Ca(NO_3)_2$]	**Bicarbonate Alkalinity (HCO_3^- mg/L)**	**Carbonate Alkalinity (CO_3^- mg/L)**	**Hydroxide Alkalinity (OH^- mg/L)**	**pH**
Pure KNO_3 (0 ppm Ca)	4.80	_	_	5.67
1 ppm Ca	6.45	_	_	6.06
2 ppm Ca	8.24	_	_	5.97

3.5 ppm Ca	7.55	_	_	6.07
6 ppm Ca	6.18	_	_	5.95
8 ppm Ca	5.49	_	_	6.05
20 ppm Ca	5.49	_	_	6.12

4.3 Results of $CaCO_3$ Contaminated KNO_3 Salt Bath

4.3.1 Compressive Stress and Depth of Layer Analysis Results

The surface compressive stress and depth of compressive stress layer for glass samples tempered in $CaCO_3$ contaminated salts are given in Figure 4.10. As a result of adding a small amount of $CaCO_3$ contamination to pure KNO_3 salt (3.5 ppm), a decrease in the compressive stress and depth of layer was observed. As the amount of $CaCO_3$ addition gradually increased, the depth of layer remained almost constant, while the compressive stress value further decreased. The surface compressive stress dropped below the expected stress range with the addition of 20 ppm $CaCO_3$. As it can be understood from here, the presence of $CaCO_3$ impurity in the specified amounts in the chemical tempering salt somewhat limited the Na^+-K^+ ion exchange but did not completely prevent it.

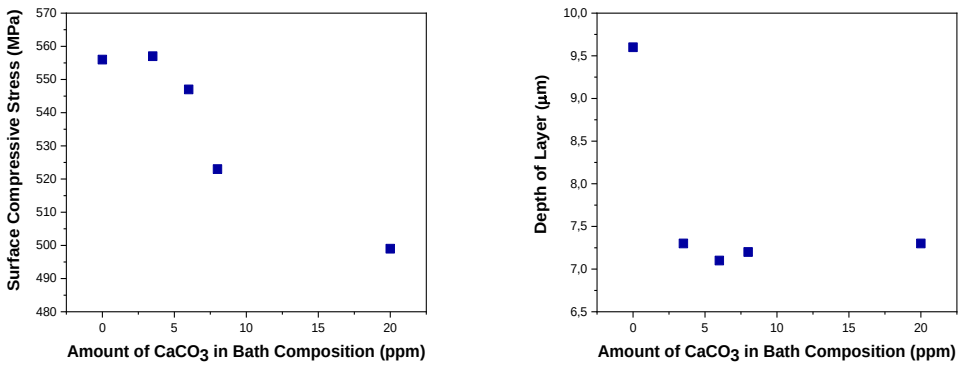


Figure 4.10 Variation of CS and DOL values for glasses tempered in different amounts of $CaCO_3$ contaminated KNO_3 salt bath

4.3.2 Vickers Hardness Test Results

The results of Vickers Hardness test applied to investigate the surface hardness of glass samples chemically tempered in $CaCO_3$ added salts are given in Figure 4.11. When the graph is examined, it is seen that the Vickers hardness values of the samples decrease with the increase in the amount of $CaCO_3$ in the tempering salt.

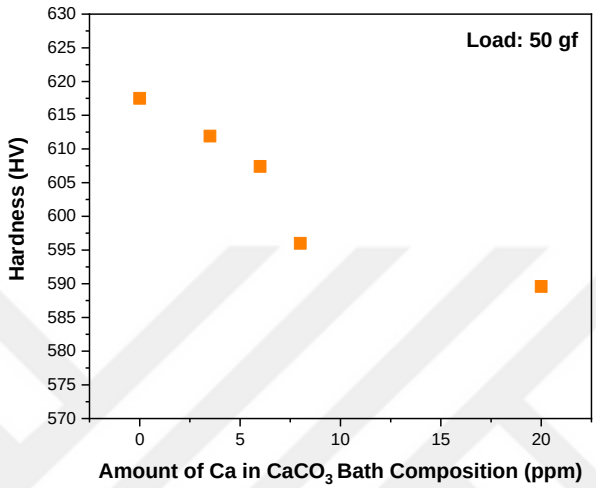
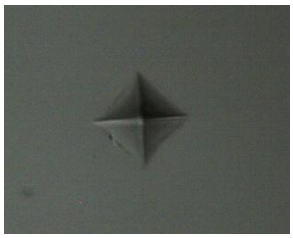
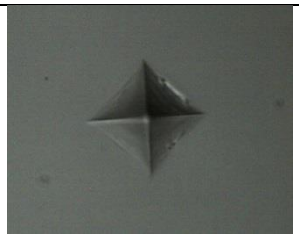
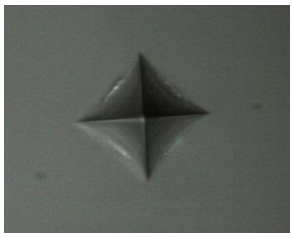
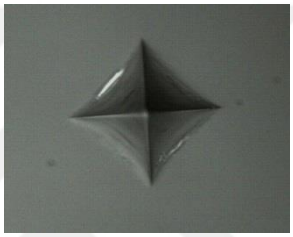
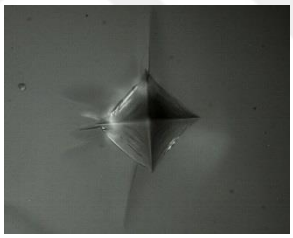


Figure 4.11 Vickers hardness test results of glass samples chemically tempered in different amounts of $CaCO_3$ containing salts

Table 4.5 shows the crack formation behavior of glass sample chemically tempered in 8 ppm $CaCO_3$ contaminated salt bath under 100, 200, 300, 500 and 1000 g loads.

Table 4.5 Crack formation behaviors of glass sample chemically tempered in 8 ppm $CaCO_3$ contaminated salt bath

Load, g	Micrographs
100	
200	

	
300	
500	
1000	

4.3.3 Ring-on-Ring Test Results

The average load values at the breaking point determined as a result of the ring-on-ring test of glass samples chemically tempered in pure KNO_3 and 8 ppm $CaCO_3$ contaminated salts are 1910 N and 1657 N, respectively. The load value of the glass sample, which was tempered in 8 ppm $CaCO_3$ added salt, at the moment of breaking decreased slightly compared to the glass sample tempered in pure KNO_3 salt bath.

4.3.4 Structural Analysis Results

IR spectroscopy graphs of glass samples chemically tempered in salt contaminated with 8 ppm $CaCO_3$ before and after aging process are given in Figure 4.12. It was observed that there was no significant change in the band structure of the glass samples before aging. After the aging process, no significant change was observed for glass samples chemically tempered in salts containing less than 8 ppm $CaCO_3$, while a small amount of change was observed for glass samples tempered in salt containing 8 ppm $CaCO_3$. As can be seen from the graphs drawn for the post-aging process, the peak corresponding to 1060 cm^{-1} wavenumber representing Si–O–Si bond vibration showed a slight shift to lower wavenumber (1057 cm^{-1}) compared to the glass samples chemically tempered in pure KNO_3 salt bath and original glass. In the band position representing the Si–O NBO vibration, it was determined that there is a beginning of shoulder formation. From here, it is understood that the glass sample is in the 1st stage corrosion state.

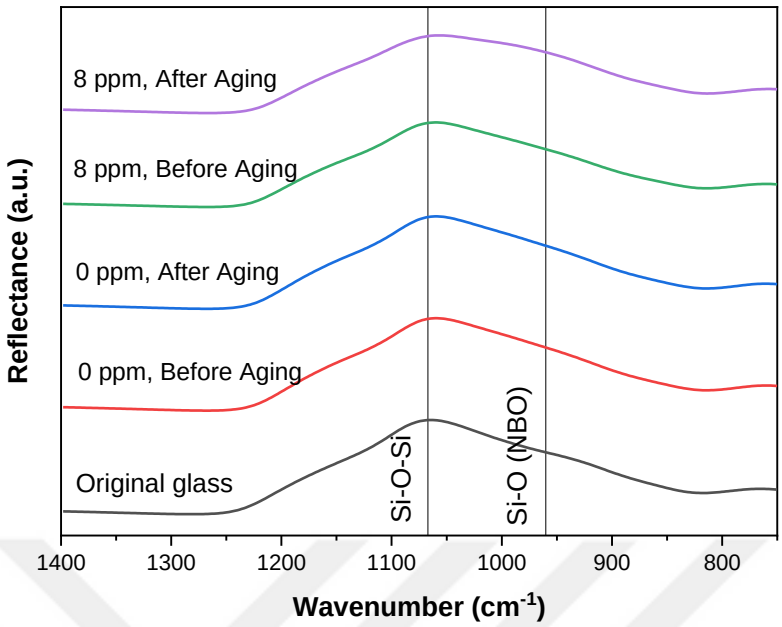


Figure 4.12 FTIR spectra of original glass and glasses chemically tempered in pure (0 ppm) and $CaCO_3$ contaminated (8 ppm) KNO_3 salt bath before and after aging process

4.3.5 Macro Examination

Macro photographs of glass samples chemically tempered in $CaCO_3$ added salts after the aging process are given in Figure 4.13. Looking at the photographs, it is seen that increasing the amount of $CaCO_3$ addition in the salt causes some deterioration in the surface of glass samples tempered in these salts after the aging process. This deterioration appeared as slight stains.

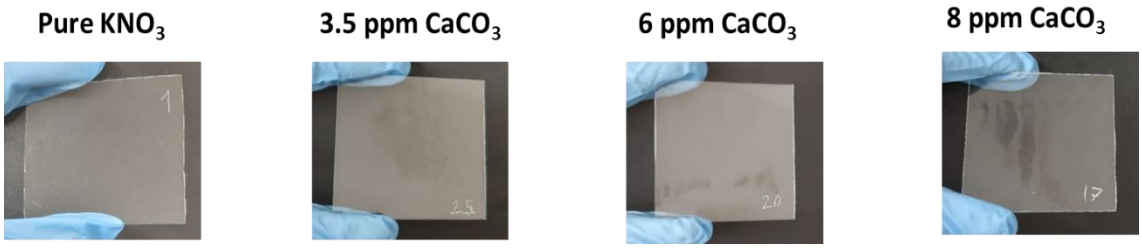


Figure 4.13 Macro photos of aged glass samples chemically tempered in different amounts of $CaCO_3$ containing salt baths

Macro photographs of glass samples chemically tempered in different amounts of $CaCO_3$ added salts after methylene blue test are given in Figure 4.14. According to the results, corrosion started to be evident on the surface with 8 ppm $CaCO_3$ addition after aging.

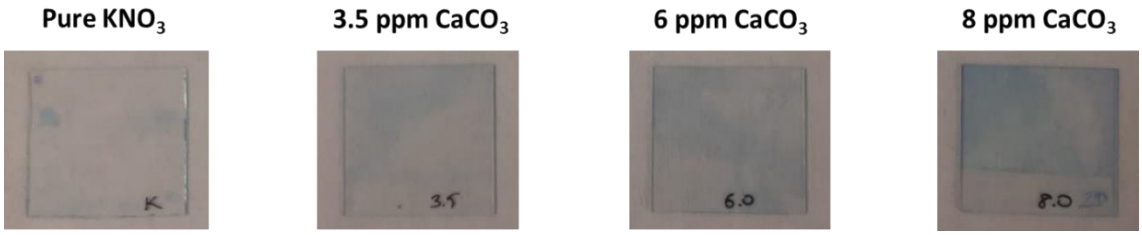


Figure 4.14 Macro photos of glass samples chemically tempered in different amounts of $CaCO_3$ containing salt baths after methylene blue test

4.3.6 Optical Analysis Results

Transmittance and haze results of glass samples tempered in $CaCO_3$ added salts before and after aging process are given in Figure 4.15. As can be seen from the figures, there was no significant change in the haze and transmittance values of the glass samples before and after the aging process.

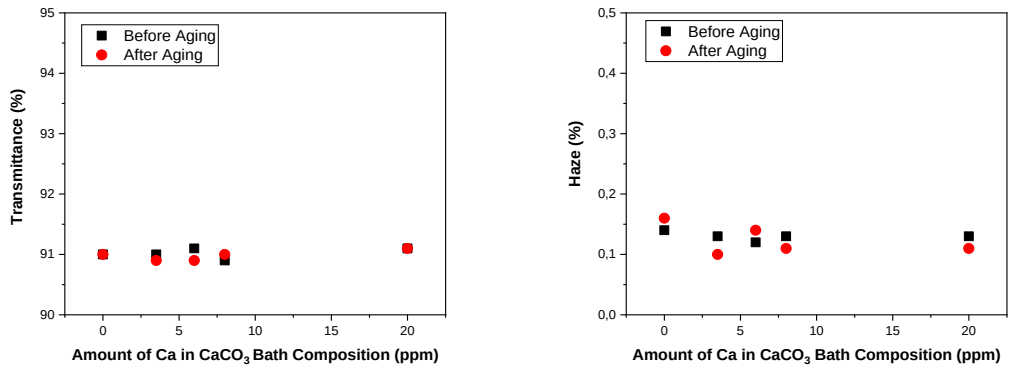


Figure 4.15 Transmittance and haze results of glasses chemically tempered in different amounts of $CaCO_3$ contaminated salt baths

4.3.7 pH and Alkalinity Analysis Results

With the addition of $CaCO_3$ impurity to the salts, the pH and bicarbonate alkalinity values increased slightly compared to the values of pure KNO_3 salt. However, since

the alkalinity depends only on the bicarbonate, it was observed that addition of $CaCO_3$ did not create a highly corrosive environment creating a significant haze on the surface of the glass but caused a corrosion in the form of staining on the surface (see Table 4.6).

Table 4.6 pH and alkalinity test results for different amount of $CaCO_3$ added salts

Bath Composition [$CaCO_3$]	**Bicarbonate Alkalinity (HCO_3^- mg/L)**	**Carbonate Alkalinity (CO_3^- mg/L)**	**Hydroxide Alkalinity (OH^- mg/L)**	**pH**
Pure KNO_3 (0 ppm Ca)	4.80	_	_	5.67
3.5 ppm Ca	6.13	_	_	6.02
6 ppm Ca	6.18	_	_	6.02
8 ppm Ca	6.86	_	_	6.63
20 ppm Ca	8.24	_	_	6.9

4.4 Results of CaO Contaminated KNO_3 Salt Bath

4.4.1 Compressive Stress and Depth of Layer Analysis Results

The surface compressive stress and the depth of compressive stress layer results of the glass samples chemically tempered in different amounts of CaO added salts are given in Figure 4.16. With the addition of a small amount (3.5 ppm) of CaO to the pure KNO_3 salt bath, the average depth of compressive stress layer decreased significantly, while the surface compressive stress increased slightly. As a result of the increase in the amount of CaO in the salt, there was no significant decrease in the depth of layer. It was observed that the compressive stress, which increased initially, decreased with the increasing amount of CaO and reached a point that the device could not measure at 20 ppm.

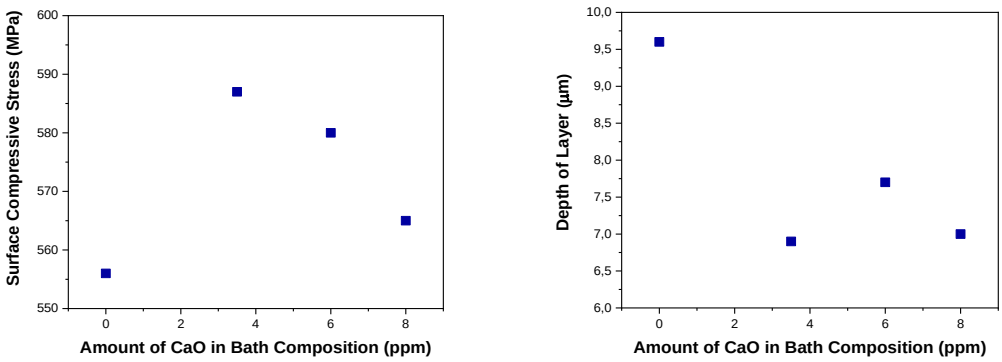


Figure 4.16 Variation of CS and DOL values for glasses tempered in different amounts of CaO contaminated KNO_3 salt bath

4.4.2 Vickers Hardness Test Results

Surface hardness values of glass samples chemically tempered in salts containing different amounts of CaO are given in Figure 4.17. According to the figure, the increase in the amount of CaO in the tempering salt caused some decrease in the surface hardness of the samples.

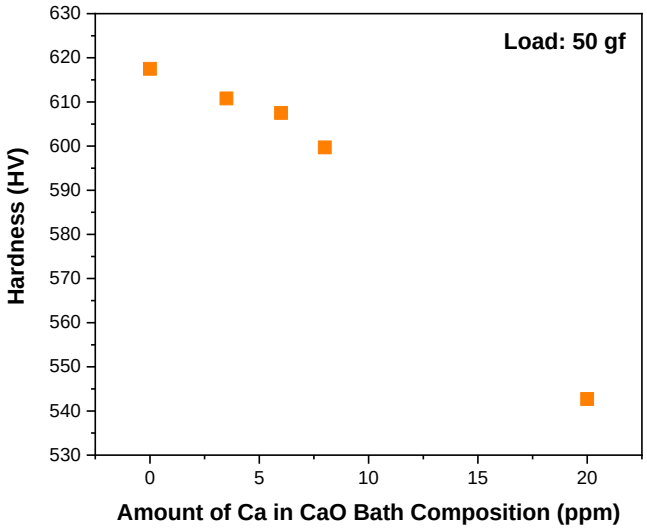
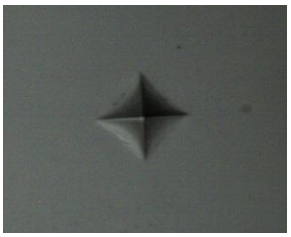
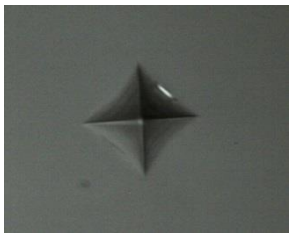
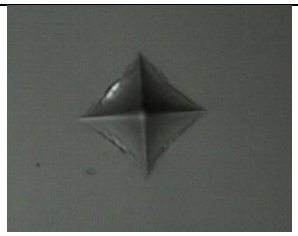
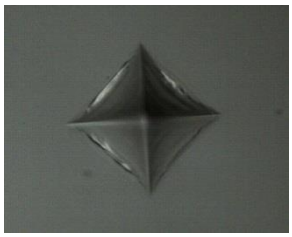
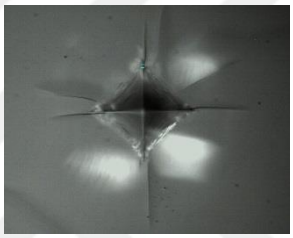


Figure 4.17 Vickers hardness test results of glass samples chemically tempered in different amounts of CaO containing salts

Table 4.7 shows the crack formation behavior of glass sample chemically tempered in 8 ppm CaO contaminated salt bath under 100, 200, 300, 500 and 1000 g loads.

Table 4.7 Crack formation behavior of glass sample chemically tempered in 8 ppm CaO contaminated salt bath

Load, g	Micrographs
100	
200	

300	
500	
1000	

4.4.3 Ring-on-Ring Test Results

The result obtained as a consequence of the ring-on-ring test applied to investigate the effect of CaO contamination on the load value at break, which is one of the indicators of the mechanical behavior of the samples, is 1511 N. When the load value of the glass sample chemically tempered in salt containing 8 ppm CaO is compared with the load value at the time of breaking of the sample tempered in pure KNO_3 salt (1910 N), it is seen that there is a significant decrease in this value.

4.4.4 Structural Analysis Results

The IR Spectra of the glass sample chemically tempered in salt bath containing 8 ppm CaO before and after the aging process are given in Figure 4.18. According to the FTIR plot it is seen that the 8 ppm CaO addition did not cause a significant change before aging process in the structure of the glass sample. After the aging process, it was observed that the addition of CaO in small amounts to the chemical tempering

salt did not cause a significant change in the structure of the samples, and when 8 ppm CaO was added, it was observed that the structure started to change. As can be seen from the graph, it is seen that the wavelength of 1060 cm^{-1} corresponding to the Si–O–Si bond vibration shifted slightly to the right (1055 cm^{-1}), that is to the smaller wavenumber region after aging process. In addition, it is seen that the band position corresponding to the vibration of the Si–O non bridging oxygen bond started to give a slight shoulder, so it is understood that the 1st stage corrosion of the sample has started.

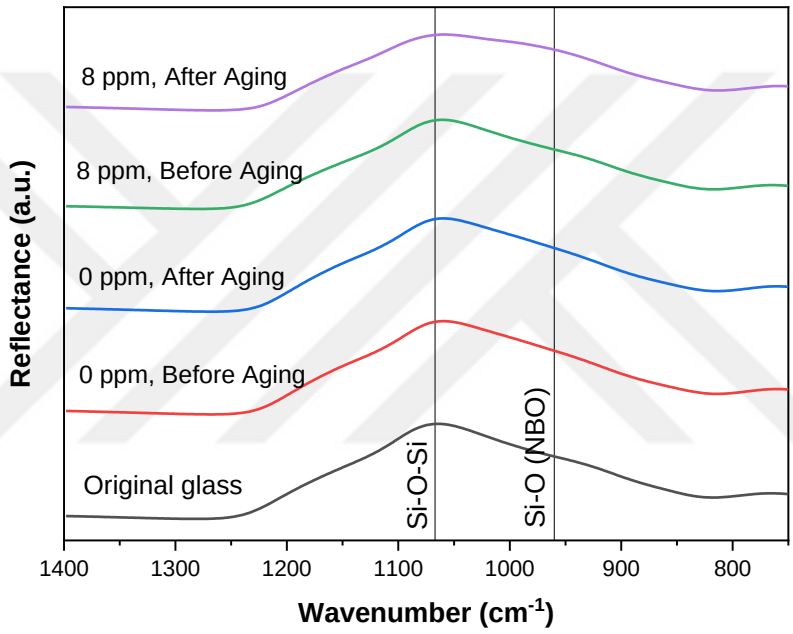


Figure 4.18 FTIR spectra of original glass and glasses chemically tempered in pure (0 ppm) and CaO contaminated (8 ppm) KNO_3 salt bath before and after aging process

4.4.5 Macro Examination

The macro images of aged glass samples chemically tempered in different amounts of CaO containing salt baths are given in Figure 4.19. While no significant difference was observed in the macro image of the glass sample chemically tempered in pure KNO_3 salt bath, the increase in CaO amount in the tempering salt caused minor deterioration on the surface appearance of glass samples.

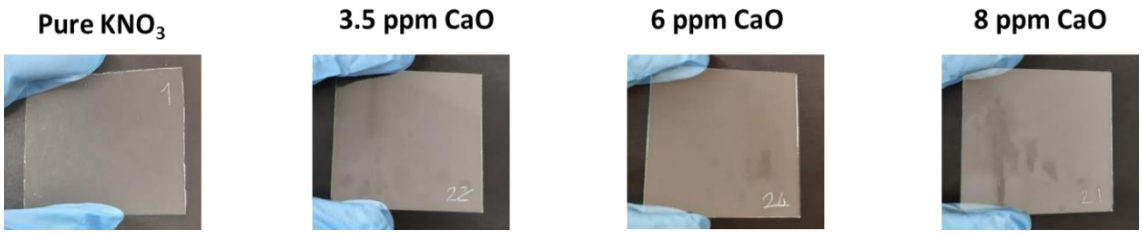


Figure 4.19 Macro photos of aged glass samples chemically tempered in different amounts of CaO containing salt baths

Macro photographs of the glass samples chemically tempered in CaO contaminated salts were taken after methylene blue test. When Figure 4.20 is examined, it was observed that while there is no obvious staining on the surface of the sample tempered in pure KNO_3 salt bath, the staining on the surface increased with the increase in the amount of CaO in chemical tempering salt.

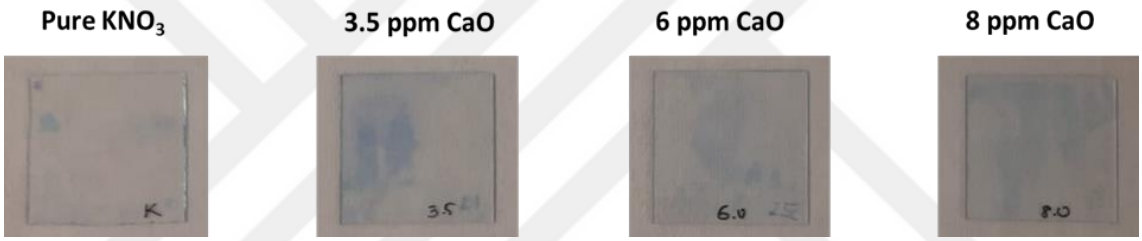


Figure 4.20 Macro photos of glass samples chemically tempered in different amounts of CaO containing salt baths after methylene blue test

4.4.6 Optical Analysis Results

The results of the transmittance and haze tests applied before and after aging process to determine the light transmittance and surface haze values of the samples are given in Figure 4.21. As can be seen, no significant changes were observed in haze and transmittance values of the samples before and after aging process.

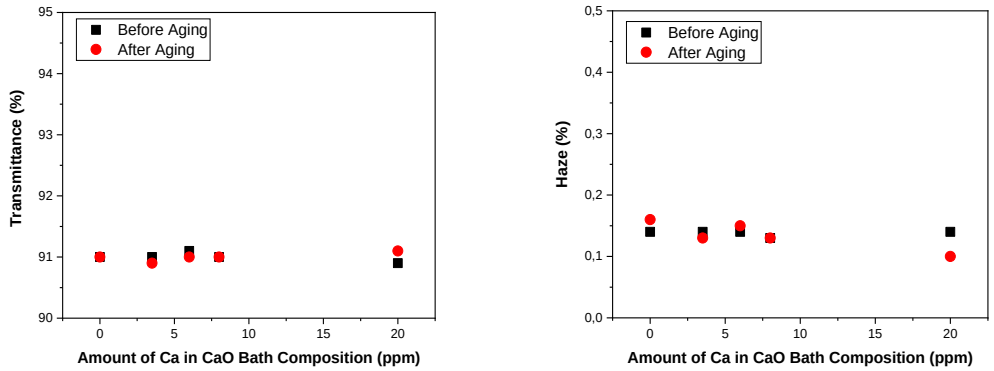


Figure 4.21 Transmittance and haze results of glasses chemically tempered in different amounts of CaO contaminated salt baths

4.4.7 pH and Alkalinity Analysis Results

Similar to other calcium contaminated baths, CaO addition did not significantly change the pH value of the salt bath, and the pH remained within acidic limits. With increasing CaO amount, a slight increase in bicarbonate alkalinity was observed, but since alkalinity is only dependent on bicarbonate, it is understood that the glass surface did not create an environment that can create serious corrosive effects (see Table 4.8).

Table 4.8 pH and alkalinity test results for different amounts of CaO added salts

Bath Composition [CaO]	**Bicarbonate Alkalinity (HCO_3^- mg/L)**	**Carbonate Alkalinity (CO_3^- mg/L)**	**Hydroxide Alkalinity (OH^- mg/L)**	**pH**
Pure KNO_3 (0 ppm Ca)	4.80	_	_	5.67
3.5 ppm Ca	6.18	_	_	6.01
6 ppm Ca	6.86	_	_	6.05
8 ppm Ca	6.86	_	_	6.32

20 ppm Ca	7.55	_	_	6.31

4.5 Discussion

4.5.1 Evaluation of Compressive Stress and Depth of Layer Analysis Results

Compressive stress and depth of layer values of glass samples chemically tempered in pure KNO_3 and different calcium contaminated salts are given in Table 4.9.

It was observed that addition of a small amount of $Ca(NO_3)_2$ impurity (1 ppm) to the pure KNO_3 salt bath decreased the CS and DOL values from 556 MPa to 540 MPa and 9.6 μm to 7.1 μm, respectively. With increasing amount of $Ca(NO_3)_2$ contamination in the salt bath, CS values of the samples showed a further decrease until the contamination amount reached to 20 ppm. On the other hand, with increasing amount of $Ca(NO_3)_2$ contamination no dramatic change was detected in DOL values. At 20 ppm contamination amount CS and DOL values decreased to a value that the device could not measure.

Considering the results of the samples chemically tempered in salts contaminated with $CaCO_3$ impurity, it was observed that a small amount of $CaCO_3$ impurity (3.5 ppm) addition to the salt decreased the CS and DOL values from 556 MPa to 550 MPa and 9.6 μm to 7.3 μm, respectively. With increasing $CaCO_3$ contamination amount, the compressive stress continued to decrease and reached down to 499 MPa at 20 ppm which fell below the expected CS value range. Although the CS values decreased, it is seen that the depth of layer values did not show a significant change with increasing $CaCO_3$ amount.

The addition of CaO impurity to the chemical tempering salt initially increased the CS value up to 587 MPa for 3.5 ppm contamination, while further increasing the amount of CaO decreased the surface CS values down to 565 MPa (for 8 ppm). However, this value was still higher than the CS value of glasses chemically tempered in pure KNO_3 salt bath. With the addition of 20 ppm CaO, CS value became too low for the FSM device to measure. Considering the effect of this form of contamination on the depth of layer, although it initially decreased the DOL value

similar to the results obtained in other calcium contamination forms, it did not create a significant change in the DOL values with further increment of CaO contamination.

Table 4.9 CS and DOL results of glasses chemically tempered in different calcium contaminated salts

Impurity Type	Ca (ppm)	Avg. CS (MPa)	Avg. DOL (μm)
No impurity (pure KNO_3)	0	556	9.6
$Ca(NO_3)_2$	1	542	7.1
	2	535	7.6
	3.5	512	7.2
	6	513	7.5
	8	472	7.4
	20	**No Value**	**No Value**
$CaCO_3$	3.5	550	7.3
	6	547	7.1
	8	523	7.2
	20	499	7.3
CaO	3.5	587	6.9
	6	580	7.7
	8	565	7.0
	20	**No Value**	**No Value**

If the results of glass samples chemically tempered in different types of calcium contaminated salts are evaluated all together, it can be said that $Ca(NO_3)_2$, $CaCO_3$ and CaO impurity forms generally reduce the compressive stress and decrease the depth of layer values compared to pure KNO_3 salt. However, depth of layer values do not show a steady decrease with increasing contamination amounts and remain at an almost constant depth. In salts contaminated with $CaCO_3$ impurity, it was observed that as the amount of impurity increases, the CS value decreases and decreases to a point below the expected surface compressive stress value at 20 ppm.

From this, it can be concluded that the CaO impurity reduces the chemical tempering efficiency by somewhat limiting the Na^+-K^+ ion exchange that should take place between the glass and salt. Compressive stress values of glasses chemically tempered in $Ca(NO_3)_2$ and CaO impurities decreased to a certain point as the amount of contamination increased, and when the amount of 20 ppm was reached the value could not be read on the device. As the reason for this, $Ca(NO_3)_2$ and CaO impurities are considered to limit the Na^+-K^+ ion exchange and prevent it completely after a certain ppm amount. The effects of $Ca(NO_3)_2$, $CaCO_3$ and CaO impurities on the depth of layer values were found to be similar, although these three impurities initially decreased the depth of layer compared to the pure KNO_3 salt, however further increase in their amount did not cause significant change in the depth of layer.

Na^+-K^+ ion exchange, which is the basic mechanism of chemical tempering process, takes place by replacing the smaller Na^+ ions in soda-lime silicate glass by the larger K^+ ions in the KNO_3 salt bath and thus creating a compressive stress on the surface. When the results of the surface stress analysis are evaluated, it can be concluded that as a result of the presence of calcium impurities in the salt, even in small amounts, the displacement of Na^+ ions in the network of the glass and K^+ ions in the salt is restricted or prevented. Since Na^+ ions in the glass and the smaller Ca^+ ions are exchanged, the compressive stress provided by the introduction of larger ions into smaller spaces cannot be created. Considering the reasons of Ca^+ ions passing from salt bath to glass instead of K^+ ions, it can be concluded that the ion exchange of Na^+-Ca^+ is thermodynamically more preferable than Na^+-K^+ ion exchange due to reasons such as lower ionic radius of Ca^+ and high ion mobility.

The depth of layer values, which is an indicator of how far the exchanged ions move from the sample surface to the center decreased initially compared to pure KNO_3 salt but did not change significantly with the increase in the amount of impurities. Based on this result, it can be concluded that calcium impurities prevent movement of exchanged ions from the surface to the center of the sample, but this occurs regardless of the amount of impurities. Since the movement of the exchanged ions from the sample surface towards the center occurs by diffusion, it can be said that all calcium impurity forms reduce the diffusion when they are first added, but

further increase in their amount does not have a dramatic effect on the diffusion process.

4.5.2 Evaluation of Vickers Indentation Test Results

The results of Vickers hardness tests applied to glasses chemically tempered in different calcium contaminated salts are given in Table 4.10.

Although it was observed that $Ca(NO_3)_2$ addition to chemical tempering salt initially increased the hardness value to 623 HV, as the amount of $Ca(NO_3)_2$ further increased the hardness values showed a decrease down to 611 HV.

The hardness values of glasses chemically tempered in $CaCO_3$ and CaO contaminated salts showed a decrease from the beginning, and as the amount of these contaminants increased, the hardness values continued to decrease reaching down to 589 HV and 542 HV for $CaCO_3$ and CaO, respectively.

There is a relationship between the surface hardness and the compression stress created on the surface of the samples. As the compression stress values of the samples decrease, the surface hardness values also decrease. The results obtained from this study also support that there is a linear relationship between surface hardness and compression stress values.

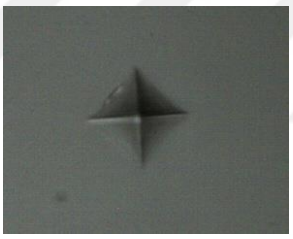
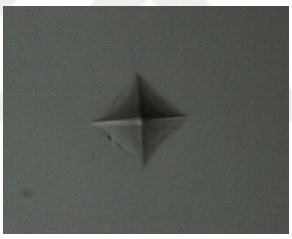
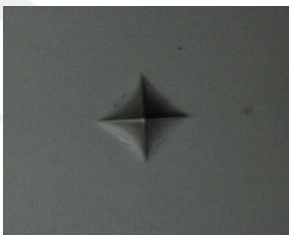
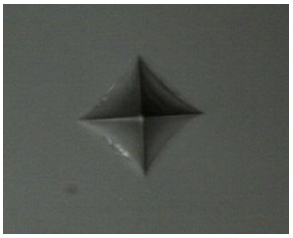
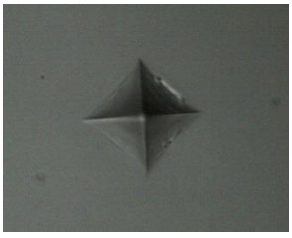
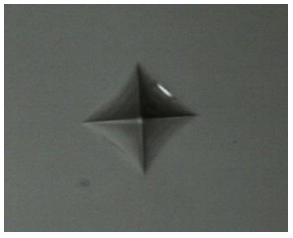
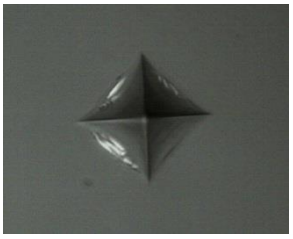
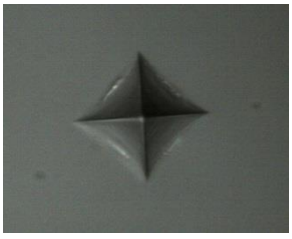
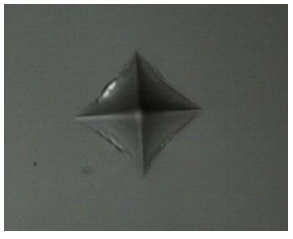
Table 4.10 Vickers indentation results of glasses chemically tempered in different calcium contaminated salts

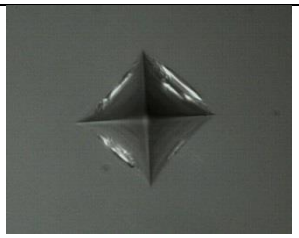
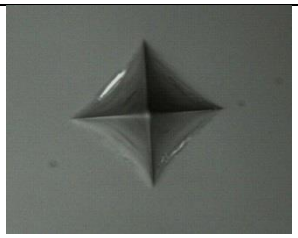
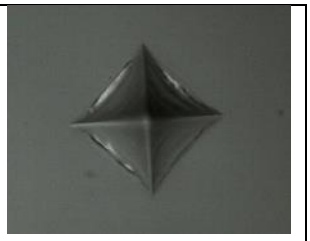
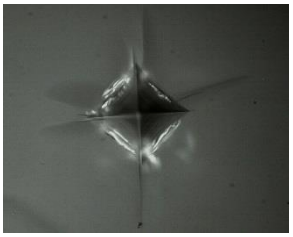
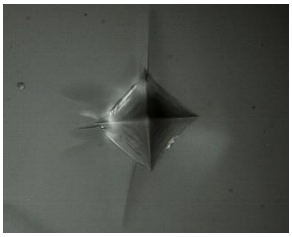
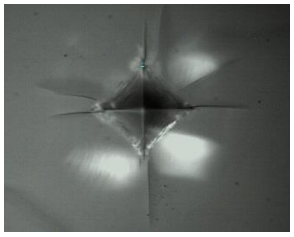
Impurity Type	Ca (ppm)	Average Hardness (HV)
No impurity (pure KNO_3)	0	617
$Ca(NO_3)_2$	1	623
	2	621
	3.5	619
	6	617
	8	614
	20	611
$CaCO_3$	3.5	612
	6	607
	8	596
	20	589

CaO	3.5	610
	6	607
	8	599
	20	542

In addition, crack formation probabilities of glasses were investigated. As a result of the Vickers tests performed using the loads of 100, 200, 300, 500 and 1000 g, crack forming behaviors of glasses are given in Table 4.11. For this test, samples chemically tempered in 8 ppm calcium containing salts were used since 8 ppm is the most critical impurity amount that limits the ion exchange between the salt and glass.

Table 4.11 Crack formation behavior of glasses chemically tempered in 8 ppm Ca^{2+} containing salts

Load, g	**Indentation Images**		
	8 ppm $Ca(NO_3)_2$	**8 ppm $CaCO_3$**	**8 ppm CaO**
100			
200			
300			
500			

			
1000			

Glasses chemically tempered in $Ca(NO_3)_2$, $CaCO_3$ and CaO contaminated salts formed cracks when the applied load was 1000 g.

4.5.3 Interpretation of Ring-on-Ring Test Results

The average breaking loads of glasses chemically tempered in pure KNO_3 and different calcium contaminated salts containing 8 ppm Ca^{2+} impurity are given in Figure 4.22.

According to the ring-on-ring test results realized to examine the fracture mechanics of glasses, it was seen that the average breaking load value for glasses tempered in pure KNO_3 salt was 1910 N and breaking loads showed a decrease for glasses tempered in salts contaminated with 8 ppm calcium impurities in different compound forms. Breaking loads decreased to 1657 N with the addition of 8 ppm $CaCO_3$, to 1511 N with the addition of 8 ppm CaO, and to 1288 N with the addition of 8 ppm $Ca(NO_3)_2$. When the effects of these three different calcium impurities on breaking loads are compared, if the order is made from the least lowered to the most lowered, the result is as follows: $CaCO_3 > CaO > Ca(NO_3)_2$.

Comparing breaking loads with compressive stress values it was observed that similar to ring-on-ring test results, $Ca(NO_3)_2$ showed the lowest compressive stress value with 472 MPa, while $CaCO_3$ and CaO had higher compressive stress values as 523 MPa and 565 MPa, respectively.

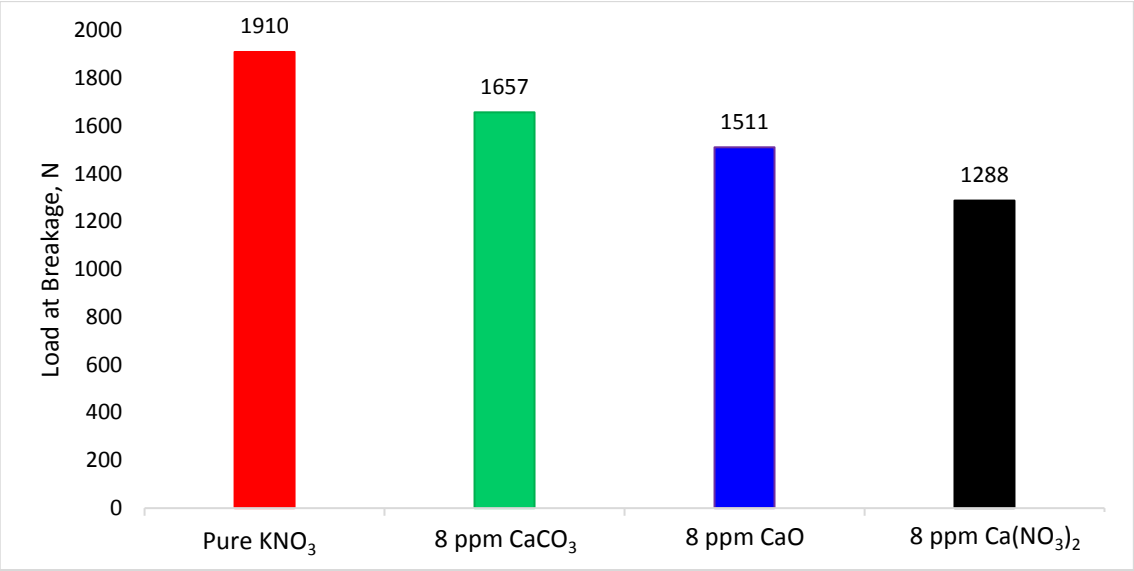


Figure 4.22 Breaking loads for glasses chemically tempered in pure KNO_3 and different calcium contaminated salts containing 8 ppm Ca^{2+} impurity

Weibull distributions of the breaking loads are given in Figure 4.23.

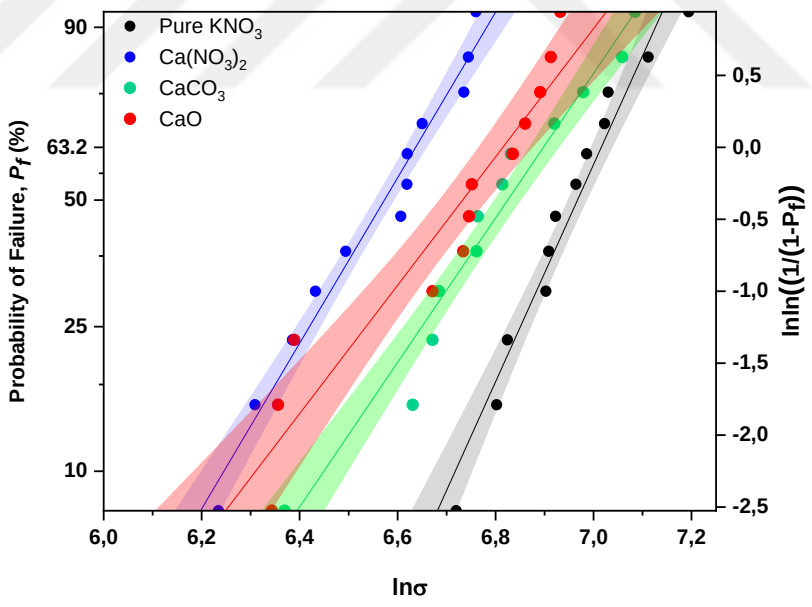


Figure 4.23 Weibull plot of glasses chemically tempered in pure KNO_3 and different calcium contaminated salts containing 8 ppm Ca^{2+} impurities

The Weibull chart is used to describe the probability of breakage of the glass for a given load value applied, allowing us to interpret the data more securely and more

accurately. The lines in the Weibull plot give the probability of failure as a function of refractive modulus or lnσ. The slopes of the lines are related to the reliability of the data series. If the deviations in the data series are low, the slopes of the lines will be high.

Considering the point where the probability of failure is 50%, glasses with the lowest mechanical performance are those that are chemically tempered in salts contaminated with $Ca(NO_3)_2$. On the other hand, glasses with the highest mechanical performance are the samples chemically tempered in pure KNO_3 followed by glasses chemically tempered in salts contaminated by CaO and $CaCO_3$ contamination, respectively.

From Weibull plots, it is seen that the data series with the highest slope belongs to pure KNO_3 followed by $Ca(NO_3)_2$, $CaCO_3$ and CaO, respectively. Based on this, the order to be made on the reliability of the data is as follows: pure KNO_3 > $Ca(NO_3)_2$ > $CaCO_3$ > CaO.

4.5.4 Evaluation of Structural Analysis

The structural analysis results of glasses chemically tempered in pure KNO_3 and different calcium contaminated salts containing 8 ppm Ca^{2+} impurity before and after aging are given in Figure 4.24.

Before the aging process (see Figure 4.24a), it is clearly seen that there is no significant difference between the structural bands of the original glass and glasses chemically tempered in pure KNO_3 and different calcium contaminated salts since there is no dramatic change in the peak corresponding to the vibrations of Si–O–Si bonds at around 1060 cm^{-1}. In addition, no shoulder formation was observed related to the vibrations of Si–O non bridging oxygen bonds. As a result, it can be said that none of the glass samples corrode after chemical tempering and before aging process.

After the aging process, FTIR spectroscopy investigations were repeated (see Figure 4.24b). While structure of original glass and glasses tempered in pure KNO_3 bath did not differ significantly after the aging process, it was concluded that there was degradation in the network structure of glass samples chemically tempered in

calcium containing salts. It was observed that the Si–O–Si vibrational bands for glass samples tempered in $Ca(NO_3)_2$, $CaCO_3$ and CaO contaminated salts showed a slight rightward shift from 1060 cm^{-1}. In addition, shoulder formation was observed for glass samples tempered in different calcium containing baths related to the vibrational bands of Si–O NBOs at around 960 cm^{-1}. The shift to the lower wavenumbers in the peaks representing the Si–O–Si vibrational bands and the shoulder formation related to Si–O vibrational bands indicate that glass samples tempered in all three different calcium containing baths were exposed to stage 1 corrosion. It can be said that the 1st stage corrosion is at the initial level since the shoulder formation is still in the initial stage and is not very clear.

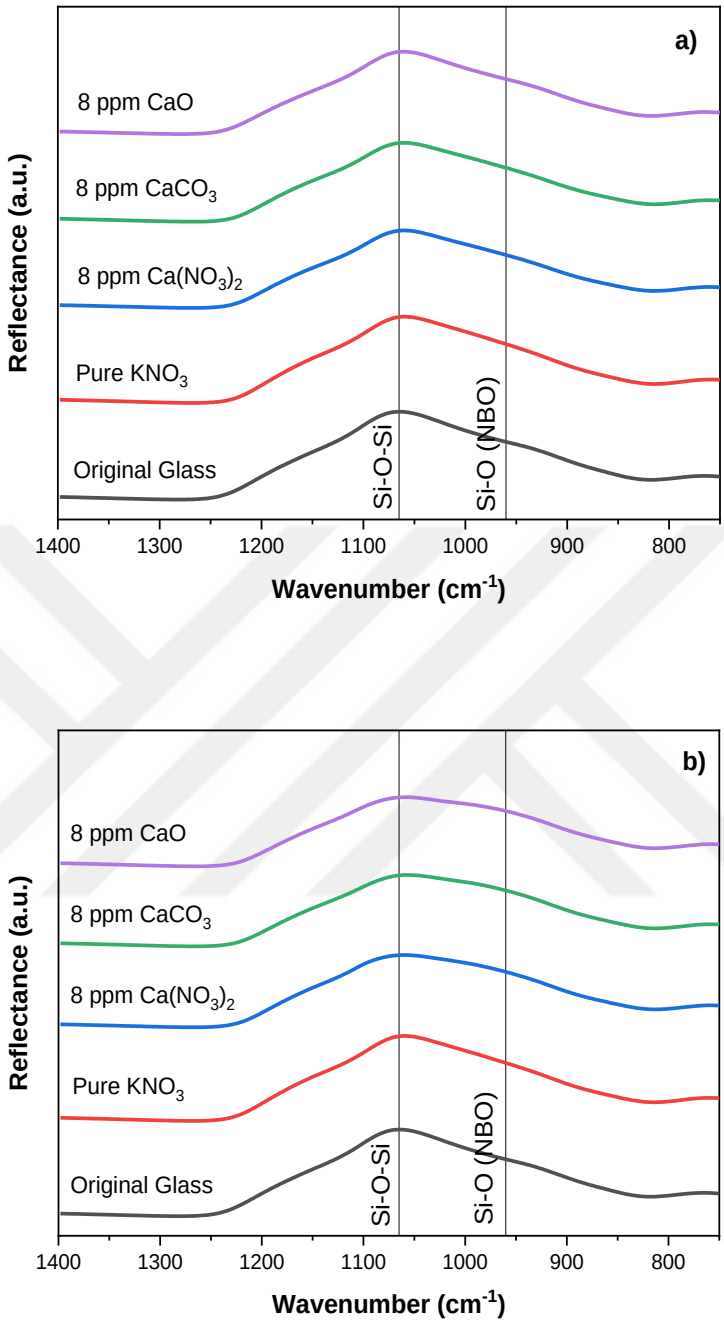


Figure 4.24 FTIR spectra of glasses chemically tempered in pure KNO_3 and different calcium contaminated salts containing 8 ppm Ca^{2+} impurity a) before and b) after aging process

4.5.5 Evaluation of Macro Examination Results

The macro photographs of chemically tempered glass samples in pure KNO_3 and different calcium contaminated salts after aging process are given in Figure 4.25. As can be seen from the photos, increasing amount of calcium impurities made atmospheric corrosion worse after the aging process. Looking at the results, it is seen that the calcium impurity that affected the surface quality most is $Ca(NO_3)_2$.

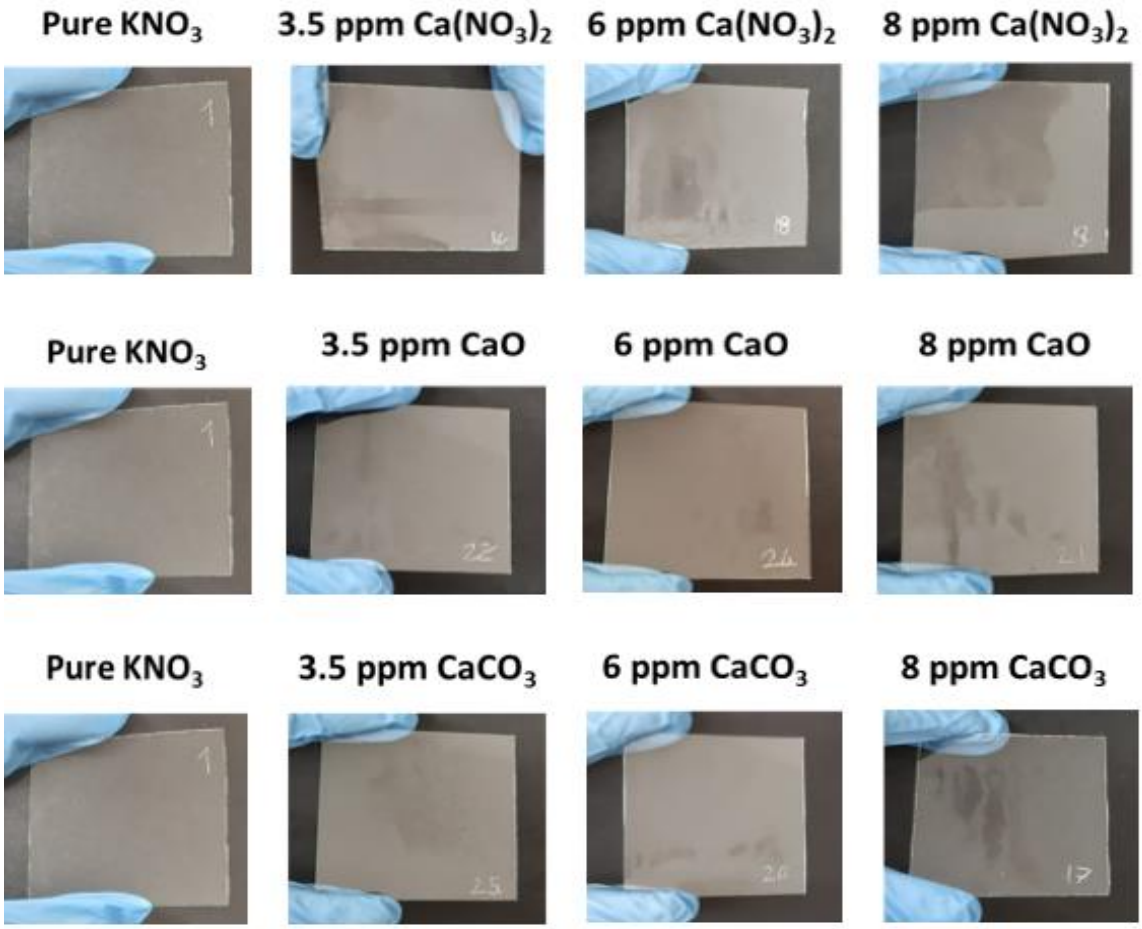


Figure 4.25 Macro images of samples after aging process

The methylene blue test results of chemically tempered glass samples in pure KNO_3 and different calcium contaminated salts after aging process are given in Figure 4.26.

After aging process, compared to the sample tempered in pure KNO_3 an increase in corrosion spots was observed for all glass samples tempered in $Ca(NO_3)_2$, $CaCO_3$ and

CaO contaminated salts. With increasing amount of contaminants these stains became more prominent. Therefore, it can be concluded that all three forms of calcium impurities slightly reduce the atmospheric corrosion resistance of glass. Evaluating the effects of different calcium containing baths on corrosion resistance of glasses it was found that $Ca(NO_3)_2$ showed the maximum negative effect, while CaO had the minimum negative effect.

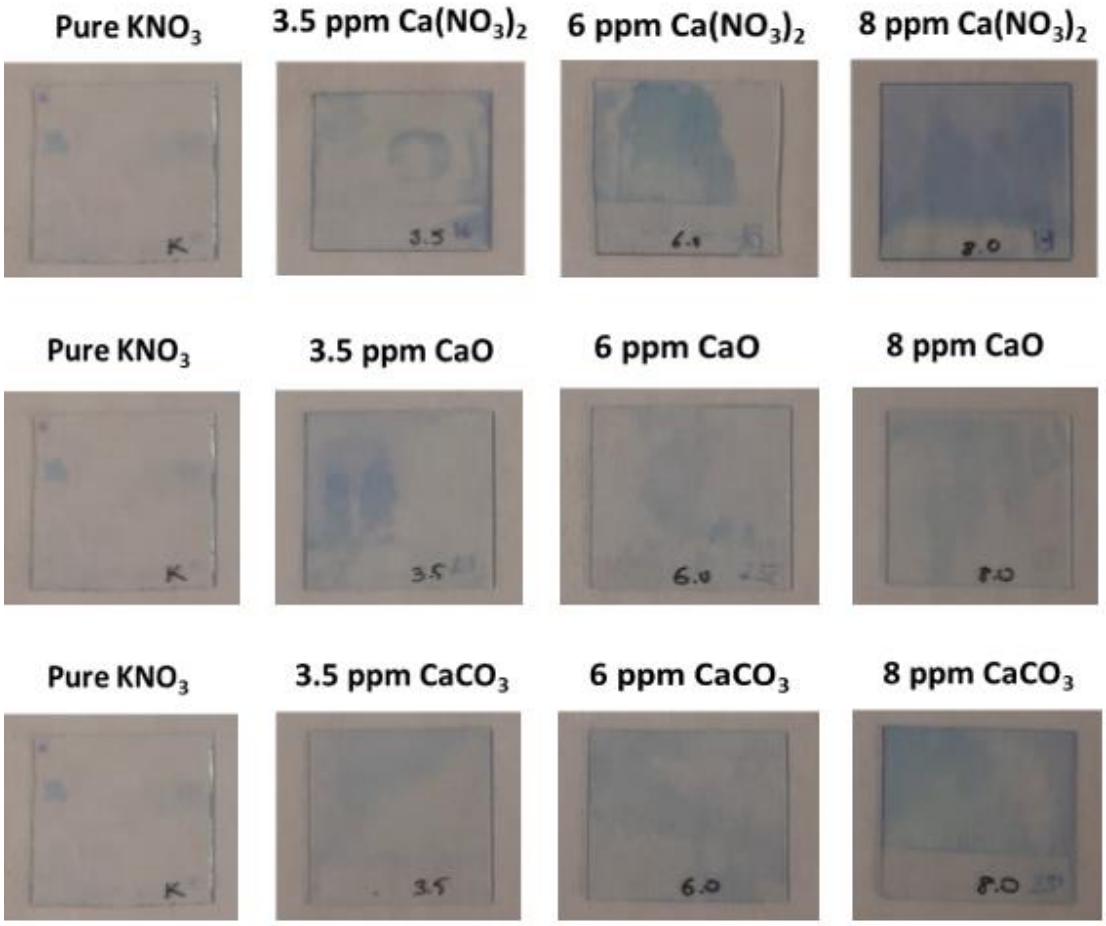


Figure 4.26 Methylene blue test results of chemically tempered glass samples after aging process

As a result of the increase in the amount of calcium in chemical tempering salt, it is known that Na^+-Ca^+ ion exchange occurs instead of Na^+-K^+ ion exchange. Since the mobility of the smaller calcium ions settling in the larger cavities of Na^+ in the glass is higher, these ions are thought to have an accelerating effect on the first stage corrosion reaction (leaching) that occurs in the glass (see Equation 2.11).

4.5.6 Evaluation of Optical Analysis Results

Transmittance and haze results of chemically tempered glass samples in different calcium contaminated salts are given in Table 4.12. As can be seen from Table 4.12, there is no significant change in the transmittance and haze values of the glass samples before and after aging. More importantly, transmittance and haze values of the original glass, glass chemically tempered in pure KNO_3 and glasses chemically tempered in calcium contaminated salts were quite similar. From this, it can be concluded that calcium impurities in the salt bath do not affect the optical properties of the chemically tempered glasses.

Table 4.12 Transmittance and haze results of chemically tempered glass samples in different calcium contaminated salts

Sample	Ca^{2+} (ppm)	Transmittance (%)		Haze (%)	
		Before Aging	After Aging	Before Aging	After Aging
Original Glass	0	91.1	91.1	0.10	0.20
Pure KNO_3	0	91.0	91.0	0.14	0.16
$Ca(NO_3)_2$	1	91.1	91.7	0.12	0.16
	2	90.9	91.2	0.12	0.11
	3.5	91	91	0.13	0.14
	6	91.1	90.9	0.13	0.13
	8	90.9	91.2	0.13	0.13
	20	91	91.1	0.13	0.09
$CaCO_3$	3.5	91	90.9	0.13	0.1
	6	91.1	90.9	0.12	0.14
	8	90,9	91	0.13	0.11
	20	91.1	91.1	0.13	0.11
CaO	3.5	91	90.9	0.14	0.13
	6	91.1	91	0.14	0.15
	8	91	91	0.13	0.13

	20	90.9	91.1	0.14	0.1

4.5.7 Interpretation of pH and Alkalinity Analysis

The pH and alkalinity results of different calcium contaminated salts are given in Table 4.13. Only bicarbonate alkalinity was detected for all samples and no carbonate and hydroxide alkalinity was found. For this reason, these alkalinities are not included in the table.

With the addition of $Ca(NO_3)_2$ impurity to the chemical tempering salt, it was observed that there was no significant change in the pH value and the alkalinity was found to depend only on bicarbonate. The fact that the alkalinity is bound to bicarbonate and the pH does not show a significant increase proves that $Ca(NO_3)_2$ contamination does not create alkaline properties in the salt and therefore does not cause serious corrosion damage in glass samples tempered in these salts. However, although there was no deterioration on the surface of the samples as a result of the chemical tempering process, some corrosion stains were observed on the surface after the aging process.

When the pH values of the salts contaminated with $CaCO_3$ were examined, there was not a dramatic change in the starting ppm amounts, but a slight increase was observed in the pH values with increasing contamination amount. Although there was a slight increase in the pH values, since these values remained within acidic limits, no serious deterioration was observed on the surface of the samples tempered in these salts. Alkalinity, on the other hand, supports the conclusion that no corrosion occurs in a way that will cause serious damage to the sample surface, since the result only depends on bicarbonate. Although no change was observed on the sample surface as a result of the chemical tempering process, it was observed that corrosion occurred on the sample surface after the aging process.

When the pH and alkalinity results of the salts contaminated with CaO were examined, small amounts of pH changes were observed as in other impurities, and alkalinity was similarly found to depend on bicarbonate. Glass samples tempered in CaO contaminated salts did not cause any visible corrosion as a result of chemical

tempering. However, similar to the results obtained in $Ca(NO_3)_2$ and $CaCO_3$ added salts, corrosion staining was observed on the sample surface after aging.

Table 4.13 pH and alkalinity results of different salt baths

Impurity Type	**Bath Composition [Ca, ppm]**	**Bicarbonate Alkalinity (HCO_3^- mg/L)**	**pH**
No Impurity Pure (KNO_3)	0 ppm Ca	4.80	5.67
$Ca(NO_3)_2$	1 ppm Ca	6.45	6.06
	2 ppm Ca	8.24	5.97
	3.5 ppm Ca	7.55	6.07
	6 ppm Ca	6.18	5.95
	8 ppm Ca	5.49	6.05
	20 ppm Ca	5.49	6.12
$CaCO_3$	3.5 ppm Ca	6.13	6.02
	6 ppm Ca	6.18	6.02
	8 ppm Ca	6.86	6.63
	20 ppm Ca	8.24	6.9
CaO	3.5 ppm Ca	6.18	6.01
	6 ppm Ca	6.86	6.05
	8 ppm Ca	6.86	6.32
	20 ppm Ca	7.55	6.31

In general, all three calcium impurities showed a similar behavior by slightly increasing the pH and alkalinity values of the chemical tempering salt. Since these values are in the acidic pH range, impurities did not cause a serious corrosion to damage the glass surfaces after chemical tempering.

The fact that no corrosion was observed on the sample surfaces after chemical tempering coincides with these results. Since calcium impurities do not have a significant effect on the pH of the salt, there is no corrosion caused by the contact of the salts containing these impurities with the surface of the glass. However, after aging the glasses tempered with salts containing these impurities, their surfaces deteriorated in direct proportion to the amount of contamination. From this, it can be concluded that calcium impurities reduce the atmospheric corrosion resistance of the glass.

4.6 General Results and Future Outlook

The essential findings of this work can be summarized as follows:

1. According to the compressive stress analysis results, the compressive stress values of glass samples chemically tempered in all calcium impurities containing baths showed a decrease compared to the samples tempered in pure KNO_3. Therefore, calcium impurities caused the compressive stress values and chemical tempering efficiency to decrease by limiting or preventing Na^+-K^+ ion exchange. This is because Na^+-Ca^+ ion exchange is thermodynamically more preferable than Na^+-K^+ ion exchange.

2. From the results of depth of compressive stress layer, it can be concluded that even small amount of calcium impurities in the chemical tempering salt causes a decrease in the stress depth values of glasses compared to the samples tempered in pure KNO_3 salt. According to this result, it can be concluded that calcium impurities in all forms limited the diffusion. However, increase in the amount of calcium impurities did not significantly change the depth of layer. Although the presence of calcium impurities in salt limits the diffusion compared to pure KNO_3 salt, this result is almost independent of the amount of calcium impurities.

3. As a result of the mechanical analysis performed on glass samples, it was concluded that the presence of calcium impurities in the chemical tempering salt caused a decrease in the hardness and fracture load values of the glass samples. Thus, it is seen that the mechanical properties of samples chemically tempered in calcium impurities containing salts are weakened. The reason for this is thought to be that calcium impurities reduce the compressive stress.

4. According to the structural analysis, it is observed that there is no significant change in the bond structure of glass samples after chemical tempering before aging. This means that before the aging process, the structural analysis results of original glass, chemically tempered glass in pure KNO_3 salt, and glass tempered in salts containing calcium impurities are similar. It is concluded that neither pure KNO_3 salt nor salts containing calcium impurities cause corrosion on the surface of the glass during the chemical tempering process. However, after the aging process, the deterioration in the bond structure of glasses tempered in different calcium impurities containing baths indicates that these impurities reduce the atmospheric corrosion resistance. How and why calcium impurities reduce atmospheric corrosion resistance require further investigation.

5. According to the macro images of the glass samples after the aging process, it was observed that for all forms of calcium contaminants deterioration in the surface appearance of the samples increased with the increase in the amount of calcium impurity.

6. When the samples tempered in salts contaminated with calcium impurities were compared with glasses tempered in pure KNO_3 and original glass, it was observed that there is no significant change in optical transmittance and haze values. Calcium impurities did not create significant changes in terms of optical properties, although they slightly impaired the surface quality.

7. As a result of the chemical analysis of chemical tempering salts, it is seen that calcium impurities cause a small increase in the pH values of the salt, since these pH values do not exceed the acidic limits and alkalinity only depends on bicarbonate. Therefore, it is concluded that the samples chemically tempered in these salts do not cause great damage to the surface.

8. In the next studies, researches should be carried out to eliminate the negative effects of the impurities in the chemical tempering salt. In this context, some trials were made by adding Al_2O_3 and silicic acid to the contaminated salt bath and positive results were observed. These studies to eliminate contamination effects should be studied in a more comprehensive and detailed manner.

REFERENCES

[1] Karlsson, S., Jonson, B., & Stålhandske, C., ''The technology of chemical glass strengthening–a review.,'' Glass Technology-European Journal of Glass Science and Technology Part A, 51(2), 41-54, 2010

[2] Varshneya, A.K., Fundamentals of Inorganic Glasses. Society of Glass Technology, 2006.

[3] Shelby, J.E., Introduction to Glass Science and Technology. Royal Society of Chemistry, 2005.

[4] Ernsberger, F. M. (1975). Bull. Am. Ceram. Soc. 54, 533.

[5] Vogel, W., Glass Chemistry. Springer-Verlag Berlin Heidelberg, 1994.

[6] Talimian, A. (2016). Strengthening of Soda-Borosilicate Glasses by Ion Exchange Processes, University of Trento, Italy.

[7] O. Richmond, W.C. Leslie, H.A. Wreidt, Trans. ASM 57 (1964) 294.

[8] Tyagi, V. & Varshneya, A. K. Measurement of progressive stress buildup during ion exchange in alkali aluminosilicate glass. J. Non-Cryst. Solids, 1998, 238 (3), 186–92.)

[9] Kistler, S.S., Stresses in Glass Produced by Nonuniform Exchange of Monovalent Ions. Journal of the American Ceramic Society, 1962. 45(2): p. 59-68.)

[10] P. Acloque, J. Tochon, Colloquium on Mechanical Strength of Glass and Ways of Improving It, Union Scientifique Contenentale du Verre, Charlroi, Belgium, 1962. (In French.)

[11] Anna I. Fu, John C. Mauro, Mutual Diffusivity, Network Dilation, and Salt Bath Poisoning Effects in Ion-exchanged Glass, Journal of Non-Crystalline Solids 363 (2013) 199–204

[12] V.M. Sglavo, A. Quaranta, V. Allodi, G. Mariotto, Analysis of the Surface Structure of Soda Lime Silicate Glass after Chemical Strengthening in Different KNO_3 Salt Baths, Journal of Non-Crystalline Solids 401 (2014) 105–109

[13] Petty, A.V. (1972). A Study of the Strengthening of Glass by Ionic Diffusion, Georgia Institute of Technology

[14] A.K. Varshneya, I.M. Spinelli, Am. Ceram. Soc. Bull. 88 (2009) 27.

[15] Frischat, G.H., Ionic diffusion in oxide glasses. Diffusion and Defect Monograph Series, ed. Y. Adda, A.D. Le Claire, L.M. Slifkin, and F.H. Wöhlbier. 1975: Trans Tech Publications.

[16] A. Kolitsch, E. Richter, Silikattechnik 32 (1981) 311.

[17] X. Zhang, O. He, C. Xu, Y. Zheng, J. Non-Cryst. Solids 80 (1986) 313.

[18] Sglavo, V.M., Chemical Strengthening of Soda Lime Silicate Float Glass: Effect of Small Differences in the KNO_3 Bath. International Journal of Applied Glass Science, 6 [1] 72–82 (2015)

[19] Demir B., Effect of Salt Baths Additive with Different Sodium Compounds on Chemical Tempering Efficiency (Master Thesis), Yıldız Technical University, Istanbul, Turkey, 2020.

[20] Karlsson, S., '' Modification of float glass surfaces by ion exchange,'' (Doctoral Thesis), Linnaeus University, Växjö, Sweden,2012.

[21] Wackerow, S, ''Fabrication and Characterization of Silver-Glass Nanocomposites'', Doctor of Philosophy, University of Dundee, 2014.

[22] Karlsson, S., Ali, S., Strand, M., Chemical Strengthening of Flat Glass by Vapour Deposition, Glafo (The Glass Research Institute) and Linnaeus University, Faculty of Technology, Växjö,2014.

[23] Carter, C.B., Norton, M.G., Ceramic Materials/Science and Engineering, Springer, 2007.

[24] C. H. L. Goodman, The structure and properties of glass and the strained mixed cluster model, Physics and chemistry of glasses vol. 26, n. 1, pp 1-10, 1985.

[25] W. H. Zachariasen, The atomic arrangement in glass, Journal of American Chemical Society, vol. 54, pp 3841-3851, Oct. 1932.

[26] Rehouma, F., Aiadi, K.E., Glasses for ion exchange technology, International Journal of Comunications, Issue 4, Volume 1, 2008.

[27] Kahnt, H., (1996). "Ionic transport in glasses", Journal of Non-Crystalline Solids, 31: 203-225.

[28] Varshneya, A., (1994). Fundamentals of Inorganic Glasses, Academia Press, San Diego.

[29] Muller, J., Evaluation of HCFeMn and SiMn Slag Tapping Flow Behaviour Using Physicochemical Property Modelling and Analytical Flow Modelling, University of Pretoria, 2015.

[30] Rao, K. J., (2002). Structural Chemistry of Glasses, Elsevier, Amsterdam.

[31] Petrov, M., Glass-metal nanocomposites for photonics applications, ed: Pasanen P., Peiponen K., Kilperlainen P., Vornanen M., Publications of the University of Eastern Finland, Dissertations in Forestry and Natural Sciences No:101, Finland, 2013.

[32] Rogoziński, R., Ion Exchange in Glass-The Changes of Glass Refraction, Ion Exchange Technologies, Chapter 7.

[33] Vallet-Regi M., Ceramics for Medical Applications, Journal of the Chemical Society, Dalton Transactions, 2001, 97-108

[34] Griffith, A.A., The Phenomena of Rupture and Flow in Solids. Philosophical Transactions of the Royal Society of London - Series A, Containing Papers of a Mathematical or Physical Character, 1921. 221: p. 163-198.

[35] Griffith, A.A. The theory of rupture. in The First International Congress for Applied Mechanics. 1924. Delft, Netherlands.

[36] Clark, D., Pickrell, G., Suchicital, C.T.A., Analysis of Strength Variation in Glass Due to Ion Exchange, State University, Virginia Polytechnic Institute, Blacksburg, Virginia, 2012.

[37] Uhlman, D.R., Kreidl, N.J., Glass: Science and Technology, Vol.5, Elasticity and Strength in Glasses, Academic Press, 1980.

[38] Inglis C.E., (1913), Stresses in a Plate Due to the Presence of Cracks and Sharp Corners, Institution of Naval Architects (54th session) , pt 1, 55: 219

[39] Griffith AA (1920), Philosophical Transactions of the Royal Society London Series A 221: 163-198

[40] Griffith AA (1924) In: Proc 1st Int Congr Appl Mech, Delft. pp 55-63

[41] Trier, F., Ranke, U.,The Glass Surface and Ways of Its Modification, Munich University of Applied Science, Germany.

[42] Solinov, V.F., Ways To Strengthen Glass: Modification of the Surface Layer, Science for glass production, Glass and Ceramics, Vol. 73, Nos. 1 – 2, May, 2016.

[43] Calahoo,C., Zhang, X., Zwanziger, J.W., Nanoindentation Study of the Surface of Ion-Exchanged Lithium Silicate Glass, J. Phys. Chem. C 2016, 120, 5585−5598.

[44] Park, S., Kim, Y., You, J., Kim, S.W., Damage-free cutting of chemically strengthened glass by creation of sub-surface cracks using femtosecond laser pulses, Volume 66, Issue 1, 2017, Pages 535-538.

[45] Varshneya, A.K., "Chemical Strengthening of Glass: Lesson and Yet To Be Learned," International Journal of Applied Glass Science, 1: 131-142, 2010.

[46] McCartney, E. R. Chemical Stregthening of glass. Proc. R. Aust. Chem. Inst. 1972, 39, 175.

[47] Dinorex™, Glass For Chemical Strengthening, https://www.neg.co.jp/en/rd/topics/product-dinorex/

[48] Nordberg, M. E., Mochel, E. L., Garfinkel, H. M. & Olcott, J. S. Strengthening by ion exchange. J. Am. Ceram. Soc, 1964, 47 (5), 215–19.

[49] Kadogawa, Y. & Yamate, T. Studies on the surface structure of chemically strengthened glasses. Part 1. Some properties of ion-exchanged glasses. Tech. Rep. Kansai Univ., 1971 (12), 57–69.

[50] Shen, J. & Green, D. J. Prediction of stress profiles in ion exchanged glasses. J. Non-Cryst. Solids, 2004, 344, 79–87.

[51] Kellman, C., Markets widen for chemically strengthened glass. Glass Ind., 1987, 68 (7), 26–7.

[52] Robert, H.D., Mechanism of electrical polarization of silica glass. Appl. Phys. Lett., 2005. 87: p.

[53] Karlsson, S., Wondrackzek L., Ali, S., Johnson, B., Trends in Effective Diffusion Coefficients for Ion-exchange Strengthening of Soda Lime Silicate Glasses, 2296-8016, 2017.

[54] Mognato, E., Schiavonato, M., Barbieri, A., Pittoni, M., Process influences on mechanical strength of chemical strengthened glass, Springer International Publishing Switzerland 2016.

[55] Schulze G., Ann. Phys. (Leipzig), 40 (1913) 335.

[56] Hale D. K., Nature, 217 (1968) 1115.

[57] Mazzoldi P., Carturan, S., Quaranta, A., Sada, C., Sglavo, V.M., Ion exchange process: History, evolution and applications, Rivista Del Nuovo Cimento Vol. 36, N. 9, 2013.

[58] Crank, J., The Mathematics of Diffusion. 2nd ed. 1975: Oxford University Press.

[59] Dushman, S. and I. Langmuir. The diffusion coefficient in solids and its temperature coefficient. in American Physical Society. 1922. Washington: Physical review.

[60] Hermans, J.M., Doctoral Thesis: Diffusion in Multicomponent Silicate Glass Melts. 2004, RWTH Aachen University: Aachen.

[61] Cooper, A.R. and D.A. Krohn, ‘‘Strengthening of Glass Fibers II: Ion Exchange,’’ J. Am. Ceram. Soc., 52 [12] 665–669 (1969).

[62] Varshneya, A. K. Ion exchange: physical properties of ion-exchanged and melt-processed glasses differ. Glass Res., 2001, 10, 11 (2, 1), 21–6, 51.

[63] Ernsberger, F. M., Strengthening of Glass. Part Two. Conclusion. Glass Ind., 1966, 542–5.

[64] Inoue, T., Ohsato, N. & Hasegawa, J. Analysis of the chemical strengthening process of glass plate by stepwise method. In Tenth Int. Congr. on Glass. Kyoto, 1974.

[65] Burggraaf, A. J. & Cornelissen, J. The strengthening of glass by ionexchange. Part I. Stress formation by ion diffusion in alkali aluminosilicate glass. Phys. Chem. Glasses, 1964, 5 (5), 123–9.

[66] Donald, I.W., Review: Methods for Improving the Mechanical Properties of Oxide Glasses. Journal of Materials Science, 1989. 24(12): p. 4177-4280.

[67] Douglas, R. W.; El-Shamy, T. M. M.: Reactions of glasses with aqueous solution. J. Am. Chem. Soc. 50 (1967) no. 1, p. 1-8

[68] Bange, K.; Rauch, F.: Surface hydration of glasses and compositional changes. Glass Res. 9 (1999) no. 1, p. 4-17

[69] Hench, L. L.: Glass surface, J. Phys. Colloque C9. Suppl. 12 (1982) p. C9-625 – C9-646

[70] Lanford, W. A.; Davis, K.; Lamarche, P.: Hydration of soda-lime glass. J. Non-Cryst. Solids 33 (1979) p. 249-266

[71] Scholze, H. J.: Glass-water interactions. J. Non-Cryst. Solids 102 (1988) p. 1-10.

[72] Delgado, J.M., Restoring Medieval Stained-Glass Transparency: Use of New Task Specific Luminescent Ionic Liquids for Corrosion Crusts Removal Março 2016 Restoring Medieval Stained-Glass Transparency: Use of New Task Specific Luminescent Ionic Liquids for Corrosion Crusts Removal, Doctoral Thesis, University of Nova de Lisboa, 2016.

[73] Ethridge, E.C.: Mechanisms and kinetics of binary alkali silicate glass corrosion, 1977, Ph.D. dissertation. University of Florida, Gainesville FL.

[74] Gösterişlioğlu Y.A., Ersundu A.E., Çelikbilek Ersundu M., Sökmen İ., Investigation the Effect of Weathering on Chemically Strengthened Flat Glasses, Journal of Non-Crystalline Solids 544 (2020) 120192.

[75] C. A. Klein, "Characteristic strength, Weibull modulus, and failure probability of fused silica glass Claude," Opt. Eng., vol. 48, no. 11, pp. 1–10, 2009.

[76] J. B. Quinn and G. D. Quinn, "A practical and systematic review of Weibull statistics for reporting strength of dental materials A practical and systematic review of Weibull statistics for reporting strengths of dental materials," Dent. Mater., vol. 26, no. 2, pp. 135–147, 2010.

[77] Kah, P., Martikainen, J., Layus, P., Methods of Evaluating Weld Quality in Modern Production (Part 1), Proceedings of 16th International Conference. Mechanika. 2011.

PUBLICATIONS FROM THE THESIS

Conference Papers:

Çalı A., Demir B., Özben N., Atılgan S., Ersundu A.E., Ersundu M.Ç., Sökmen İ., ''The Effect of Different Calcium Compounds on Bath Contamination in Chemical Strengthening Process'', Şişecam International Glass Conference combined with 34th Şişecam Glass Symposium (November 21-22, 2019), page 166, Istanbul, Turkey.

Projects:

YTU Scientific Research Project (BAP) No: FYL-2019-3683 "Effect of Salt Baths Contaminated with Different Calcium Compounds on Chemical Strengthening Efficiency".